Networks and Heterogeneous Media

https://www.aimspress.com/journal/nhm

NHM, 20(2): 701–731.
DOI: 10.3934/nhm.2025030
Received: 02 March 2025
Revised: 20 May 2025
Accepted: 23 May 2025
Published: 12 June 2025

Research article

A machine learning solutions approach of a time-delayed stochastic $\tilde{S}\tilde{E}\tilde{I}\tilde{R}\tilde{V}$ model

Mostafa Zahri[1,*], Inayat khan[2], Rahat Zarin[3], Amir khan[2] and Rukhsar Ikram[2]

[1] College of Sciences, Department of Mathematics, RGs MASEP and BioInformatics FG, University of Sharjah, United Arab Emirates
[2] Department of Mathematics and Statistics, University of Swat, KPK, Pakistan
[3] Department of Mathematics, Faculty of Science, King Mongkut's University of Technology Thonburi (KMUTT), Bangkok 10140, Thailand

* **Correspondence:** Email: mzahri@sharjah.ac.ae.

Abstract: In this work, we analyze the dynamics of a stochastic $\tilde{S}\tilde{E}\tilde{I}\tilde{R}\tilde{V}$ model with a time delay. We mainly investigate the time delay's influence on these classes' asymptotic behavior. Furthermore, we examine the existence and stability of disease-free and endemic equilibrium points. To better understand the parameter's effects on the spread of an epidemic, we integrate artificial neural networks with the Bayesian regularization method. Additionally, leveraging physics-informed artificial intelligence (AI) and specialized machine training, we develop an advanced framework for solving systems of partial differential equations (PDEs). This approach enhances the accuracy of predictions and facilitates the optimal control and effective implementation of real-world epidemic management strategies.

Keywords: epidemic stochastic model; COVID-19; time delay dynamics; stochastic stability; Bayesian regularization; machine learning; artificial neural networks

1. Introduction

Mathematical modeling in epidemiology is a rapidly advancing field with extensive applications in analyzing and understanding the spread of infectious diseases. These models facilitate the study of epidemics diffusion and offer critical insights into the factors influencing disease transmission. By leveraging data from medical sciences, researchers can examine outbreak patterns and inform public health authorities about potential risks and strategies for containment.

Over the past decade, various mathematical models have been designed to describe the progression of infectious diseases, including SI, SIS, SIR, SARS, H1N1, HBV, and H5N1 models. Where SI

describes a basic disease model with only susceptible and infectious compartments, SIS extends this by allowing individuals to return to the susceptible class after infection. SIR incorporates recovery with immunity. SARS is a viral respiratory illness caused by the Corona virus. H1N1 triggered the 2009 influenza pandemic. HBV is a liver-infecting virus transmitted through blood or bodily fluids. H5N1 is an avian influenza strain with high fatality in humans; see [1, 2]. These models are instrumental in predicting the course of outbreaks and guiding decision-making processes for public health interventions [3–6]. Their primary purpose is to provide accurate forecasts and contribute to the stability of public health systems by offering a structured approach to disease analysis and control.

The foundational work of Kermack and McKendrick provided the basis for detailed studies on infectious disease modeling [7, 8]. Their research paved the way for numerous advancements, including developing the SIRS, SEIS, and SEIRS models. Where SIRS models account for temporary immunity, allowing recovered individuals to become susceptible again. SEIS includes an exposed stage before individuals become infectious, without lasting immunity. SEIRS combines an incubation period and temporary immunity, making it suitable for latency and non-permanent recovery diseases. These models have been extended to incorporate vaccination strategies, time delays, and environmental influences; see [9–11] for modeling using fractional derivatives; for models using deterministic evolutionary partial differential equations, we refer to [12–17], and for systems involving stochastic partial differential equations see [18]. Integrating solutions from the proposed complex systems enhances epidemiological models' accuracy and applicability in real-world scenarios.

The interactions among disease transmission, vaccination programs, and social behaviors have led to an interdisciplinary approach to epidemiology. Statistical epidemiology, in particular, plays a significant role in assessing an epidemic's severity and informing public health strategies. Using statistical methods, researchers can analyze infection trends, estimate transmission rates, and predict future outbreaks. These insights are crucial for implementing timely interventions and mitigating the impact of infectious diseases on communities.

Epidemics of infectious diseases can be modeled using either deterministic or stochastic approaches. Deterministic models, which are formulated as systems of ordinary differential equations (ODEs), are favored by many researchers due to their simplicity in analysis. However, these models have limitations, such as providing less detailed information, relying on the law of large numbers, and being less effective for small populations. Additionally, they fail to account for random effects that can cause deviations from the predicted trajectories. To address these limitations, stochastic modeling has emerged as an alternative. This approach incorporates random elements into the model, acknowledging that many real-world phenomena are influenced by stochastic noise, which deterministic ODE models overlook. Stochastic models, especially in heterogeneous and homogeneous populations, provide a more realistic representation of epidemic dynamics by including random terms or noise intensities through parametric perturbation techniques [19].

Over the past decade, artificial intelligence (AI) and machine learning (ML) have emerged as promising tools for addressing complex social issues by efficiently identifying patterns and integrating diverse data sources. However, traditional AI/ML methods often require extensive labeled data and may produce unreliable predictions for nonstationary systems due to a lack of mechanistic constraints. These models also struggle to distinguish true epidemic trends from data noise. Recently, AI-based solvers for differential equations have gained attention for integrating scientific laws

(ODEs/PDEs) into neural networks, enabling parameter inference from limited data by leveraging the structure of the underlying physical or biological systems [20].

This study evaluates the applicability of the $\tilde{S}\tilde{E}\tilde{I}\tilde{R}\tilde{V}$ epidemic model for COVID-19 [21]. In this model, $N(t)$ represents the total population at a given time t, which is further divided into five distinct compartments as follows:

$$\tilde{S}(t) + \tilde{E}(t) + \tilde{I}(t) + \tilde{R}(t) + \tilde{V}(t) = N(t), \tag{1.1}$$

where $\tilde{S}(t)$ represents the susceptible population, $\tilde{E}(t)$ represents the exposed (but not yet infectious) individuals, $\tilde{I}(t)$ represents the infectious population, $\tilde{R}(t)$ represents those who have recovered and gained immunity, and $\tilde{V}(t)$ represents the vaccinated individuals. The model dynamically evolves, accounting for infection rates, recovery rates, and vaccination strategies. The basic reproduction number R_0, which determines whether an outbreak will persist or decline, is a key parameter in the analysis. By incorporating time-dependent variables and intervention measures, the model provides a comprehensive framework for assessing the spread and control of COVID-19.

Mathematical modeling continues to be a vital tool in understanding and managing infectious diseases. However, integrating advanced statistical techniques, computational simulations, and machine learning approaches has significantly enhanced the predictive capabilities of epidemiological models.

AI is increasingly important in enhancing epidemiological models. AI-driven approaches, such as deep learning and neural networks, allow for more precise predictions by analyzing vast amounts of data in real time. AI can help identify early warning signals of outbreaks, optimize intervention strategies, and improve the allocation of medical resources. By leveraging AI, researchers can automate complex computations and refine the existing models to provide more dynamic and adaptable responses to emerging epidemics.

As epidemiology evolves, collaborative efforts between mathematicians, statisticians, healthcare professionals, and AI specialists will be essential in addressing emerging challenges in infectious disease control. The continued development of mathematical models, augmented by AI techniques, will play a critical role in shaping effective intervention policies, improving healthcare resilience, and safeguarding global health [20].

2. Model formulation

The starting model of our study is given as follows:

$$\begin{cases} \dfrac{d\tilde{S}}{dt} &= \Lambda - \Lambda\nu + \omega\tilde{R}(t) - \Psi\tilde{S}(t)\tilde{I}(t) - \nu_r\tilde{S}(t) - d\tilde{S}(t) - \eta\tilde{S}(t) + \sigma\tilde{V}(t), \\ \dfrac{d\tilde{E}}{dt} &= \Psi\tilde{S}(t)\tilde{I}(t) - (Q + d + l)\tilde{E}(t), \\ \dfrac{d\tilde{I}}{dt} &= Q\tilde{E}(t) - (\kappa + d + l)\tilde{I}(t), \\ \dfrac{d\tilde{R}}{dt} &= \Lambda\nu + \kappa\tilde{I}(t) - (d + \omega)\tilde{R}(t) + \nu_r\tilde{S}(t), \\ \dfrac{d\tilde{V}}{dt} &= \eta\tilde{S}(t) - \sigma\tilde{V}(t) - d\tilde{V}(t), \end{cases} \tag{2.1}$$

where

- $\eta\tilde{S}(t)$: Individuals get vaccinated and move from $\tilde{S}$ to $\tilde{V}$.
- $\sigma\tilde{V}(t)$: Immunity from vaccination wanes over time, moving individuals back to $\tilde{S}$.

Here, $\tilde{S}(t)$ is the healthy class, $\tilde{E}(t)$ is the exposed class, $\tilde{I}(t)$ is the infected class and $\tilde{R}(t)$ and $\tilde{V}(t)$ represent the dynamics of the vaccinated population whenever (t) contains the number of recovered individuals. Table 1 gives a complete overview of the parameters used in the proposed model and their definitions.

Table 1. The biological descriptions of the parameters in the model (2.1).

Parameters	Physical interpretation
Λ	Birth rate
ν	Proportion of vaccinated newborns
ν_r	Rate of vaccination of susceptible individuals
ω	Rate of transmission from recovered to susceptible class
Ψ	Rate of transmission from susceptible to exposed class
Q	Rate of transmission from exposed to infected class
κ	Recovery rate of infected individuals
d	Natural death rate or deaths from any other disease
l	Death rate due to COVID-19
η	Individuals get vaccinated and move from $\tilde{S}$ to $\tilde{V}$
σ	Immunity from vaccination wanes over time, moving individuals back to $\tilde{S}$

For epidemiological modeling of COVID-19, stochastic modeling has many advantages over classical modeling. Stochastic models can capture the randomness and uncertainty of transmission and spread of a virus. This is particularly important for COVID-19, where the dynamics of the virus and its impact on populations can vary greatly depending on factors such as demographics, age distribution, lifestyle behaviors, etc. Stochastic models also allow for more nuanced, complex modeling of interventions, which can provide valuable information for public health and policy decisions. Using stochastic modeling can provide a more accurate and comprehensive understanding of the spread of COVID-19 and its impact on populations and inform effective strategies for preventing and controlling it.

Contingency models allow nuanced, complex modeling of interventions, such as the impact of levels of social distancing measures or vaccine effectiveness. They can also include realistic assumptions about individual behaviors and contact patterns to help control the exact spread of the virus. Much more, because of this, the data provide insights. These probabilistic predictions can help inform interventions and policies that effectively identify high-risk areas. In contrast, classical models rely on fixed assumptions, which do not adequately capture virus transmission's the complex and dynamic nature of a virus transmission. Classical models can also prove that the effect of an intervention has been too weak, and it has been assumed that all individuals are equally susceptible to the virus. This can lead to incorrect predictions and ineffective interventions. Overall, using stochastic modeling in COVID-19 epidemic modeling can provide a more accurate and comprehensive understanding of the spread of the virus and its impact on populations. This could point to more effective prevention and control strategies, ultimately helping to lower the impact of the epidemic.

Models based on stochastic differential equations are more appropriate for mathematically simulating biological phenomena than their deterministic counterparts because stochastic differential equation models can add an extra layer of realism. Compared with deterministic models, stochastic ones generate more useful output because we can create a distribution of the expected results, such as the infected population size at time t, by repeatedly running a stochastic model. Contrarily, a deterministic model yields only a single predicted outcome for a given set of initial conditions [22–24].

Due to a lack of resources or sufficient time for disease observation, various infectious models cannot offer comprehensive information about the relevant disease. This means that investigating these models after all of the symptoms have appeared in human beings or after the incubation period has ended may be more instructive, as shown in [25]. The incubation period, also known as time delay, is very beneficial for producing more accurate results [26, 27]. In contrast to other problems without a time delay, delay model analysis is more complicated.

Over time, differential equations have been widely used to model biological systems, though many early models neglected the roles of randomness and time delays. Recently, there has been growing interest in stochastic delay differential equations (SDDEs), which incorporate both noise and delays to better reflect real-world dynamics. Despite their relevance, SDDEs remain underutilized due to the mathematical and computational complexity involved in solving them, often requiring specialized methods and significant resources. These equations generalize both stochastic and delay differential equations and have applications in epidemiology, ecology, control systems, and finance. Delays often represent latent processes, while stochastic components capture random influences. Ongoing research aims to improve the usability and efficiency of SDDEs in complex modeling scenarios [28]. Recently, some researchers have shown an interest in studying delay models. Bai and Wu [29] dealt with healthy, infectious, and recovered (SIR) disease models for stationary waves with nonlinear incidence. Liu et al. [30] discussed an asymptotic stochastic SIR disease model with time delay by assuming transient immunity. Additionally, non-local attraction with time delay and scale-free networking has been mathematically analyzed in the context of the SIRS disease model [31]. In our approach, however, we adopt the delay-time framework proposed by Kumar et al. [21], which captures the time required for all symptoms to appear fully. Furthermore, the model will be perturbed by incorporating Brownian motion (environmental noise) and modifying specific parameter values.

3. Stochastic model formulation

Motivated by the aforementioned discussions, we modify the system (2.1) by including the latent delay. Hence, the following time delay model will be assumed:

$$\begin{aligned}
\frac{d\tilde{S}}{dt} &= [\Lambda - \Lambda\nu + \omega\tilde{R}(t) - \Psi\tilde{S}(t)\tilde{I}(t) - \nu_r\tilde{S}(t) - d\tilde{S}(t) - \eta\tilde{S}(t) + \sigma\tilde{V}(t)]dt + \varsigma_1\tilde{S}\,dB_1(t),\\
\frac{dE}{dt} &= [\Psi\tilde{S}(t)\tilde{I}(t) - (Q + d + l)\tilde{E}(t)]dt + \varsigma_2\tilde{E}dB_2(t),\\
\frac{d\tilde{I}}{dt} &= [Q\tilde{E}(t) - (\kappa + d + l)\tilde{I}(t)]dt + \varsigma_3\tilde{I}dB_3(t),\\
\frac{d\tilde{R}}{dt} &= [\Lambda\nu + \kappa\tilde{I}(t) - (d + \omega)\tilde{R}(t) + \nu_r\tilde{S}(t)]dt + \varsigma_4\tilde{R}dB_4(t),\\
\frac{dV}{dt} &= [\eta\tilde{S}(t) - \sigma\tilde{V}(t) - d\tilde{V}(t)]dt + \varsigma_5\tilde{R}dB_5(t).
\end{aligned} \tag{3.1}$$

In this context, the notation $B_i(t); i = 1, 2, 3, 4, 5$ represents stationary and independent Brownian motions. The corresponding white noise intensities in the environment are denoted as $\varsigma_i^2; i = 1, 2, 3, 4, 5$ with each ς_i being greater than zero, having and with the initial conditions stated as follows:

$$\begin{aligned}
&\tilde{S}(t) = \phi_1(t), \qquad \tilde{E}(t) = \phi_2(t),\\
&\tilde{I}(t) = \phi_3(t), \qquad \tilde{R}(t) = \phi_4(t), \qquad -\tau \le t \le 0,\\
&\tilde{V}(t) = \phi_5(t), \quad \phi_i(t) \in C, i = 1, 2, 3, 4, 5.
\end{aligned} \tag{3.2}$$

Herein, $C : [-\tau, 0] \to \mathbb{R}_+^5$ is an integral class of Lebesgue's existing operators. This study's objectives were to analyze dynamical properties of the system's root before a disease emerges and to validate that there is at least one recurrent positive (greater than zero) solution of the time-delayed stochastic COVID-19 epidemic models.

The remainder of the paper is structured as follows: In a feasible region, the solution of the model (3.1) derived in the Section 4 is found to be positive, and the upper bound and lower bound are fixed. Additionally, the upkeep robustness of the problem under consideration and the outcomes required to lessen infection are investigated. In Section 6, reliable outcomes are obtained for the stationary distribution's dynamic behaviors. The outcomes for the stochastic model's extinction are provided in Section 5. The scheme obtained for stochastic stability through numerical simulation is illustrated in Section 7. Section 8 containing the inclusion includes a few observations regarding the conclusions and as well as future work.

4. The positive solution's qualitative analysis

Herein, with a view to investigating the dynamic behavior of the model, we point out that the system (3.1) possesses a unique non local solution in the area that is feasible.

This is possible to achieve if the system's coefficients in Eq (3.1) satisfy the growth and conditions of the Lipschitzian then one, in which case, a positive solution will exist. As a result, it can be done very easily, so we omit it. Following this, the Lyapunov operator's methods are used in order to achieve a positive and non-local solution [32–34].

Theorem 4.1 (Existence of the solution)**.** *Under the initial condition (3.2), the system* (3.1) *admits a unique positive solution* $(\tilde{S}(t), \tilde{E}(t), \tilde{I}(t), \tilde{R}(t), \tilde{V}(t))$ *in* $\mathbb{R}_+^5$ *for all* $t \ge -\tau$,. *a.s.*

Proof. With the initial solution $(\tilde{S}(0), \tilde{E}(0), \tilde{I}(0), \tilde{R}(0), \tilde{V}(0))$, the coefficients of the problem (3.1) satisfy the local Lipschitz condition, ensuring that the model (3.1) possesses a unique local solution $(S(t), E(t), I(t), R(t), V(t))$ for $t \in [-\tau, \tau_e)$ almost surely. The value τ_e represents the duration of infection. For more details, we refer to [32–34].

Since the objective of the study was to establish the non local nature of the solution, such that $\tau_e = \infty$, $k_0 \geq 1$ can be extensively large, with $(\tilde{S}(\theta), \tilde{E}(\theta), \tilde{I}(\theta), \tilde{R}(\theta), \tilde{V}(\theta) \in [\frac{1}{k_0}, k_0]$ such that $\theta \in [-\theta, 0]$. The concept of the time threshold is defined as follows $\forall k \geq k_0$ where $k \in \mathbb{N}$,

$$\tau_k = \inf\left\{t \in [-\tau, \tau_e)\{min(\tilde{S}(t), \tilde{E}(0), \tilde{I}(t), \tilde{R}(t), \tilde{V}(t)) \leq \frac{1}{k} \text{ or } \max(\tilde{S}(t), \tilde{E}(t), \tilde{I}(t), \tilde{R}(t), \tilde{V}(t)) \geq k\}\right\}. \tag{4.1}$$

Since the objective is to find that the solution will be non-local, in such a way $\tau_e = \infty$. Let $k_0 \geq 1$ be large, $(\tilde{S}(\theta), \tilde{E}(\theta), \tilde{I}(\theta), \tilde{R}(\theta), \tilde{V}(\theta)) \in [\frac{1}{k_0}, k_0]$ such that $\theta \in [-\theta, 0]$. The concept of the time break is given as: $\forall k \geq k_0$ where $k \in \mathbb{N}$, assuming $min\phi = \infty$ (The set ϕ is void). As $k \to \infty$, τ_k is increases. If, we consider $\tau_\infty = \lim_{k\to\infty} \tau_k$, then $\tau_\infty \leq \tau_e$. Hence, we going to prove that $\tau_\infty = \infty$, and thus $\tau_e = \infty$ since, $(\tilde{S}(t), \tilde{I}(t), \tilde{E}(t), \tilde{R}(t), \tilde{V}(t)) \in \mathbb{R}^4_+$ then $\forall -\tau \leq t$. Whenever $\iota \in (0, 1)$ we also have$0 < \widetilde{T}$ and $P\{\widetilde{T} \geq \tau_\infty\} > \iota$. Thus, $\exists\, k_0 \leq k_1$ where k_1 is an integer.

$$P\{\widetilde{T} \geq \tau_k\} \geq \iota \ \ \forall \ \ k \geq k_1. \tag{4.2}$$

We have taken the C^2- operator $\mathbb{V} : \mathbb{R}^5_+ \to \mathbb{R}_+$ as follows:

$$\mathbb{V}(\tilde{S}, \tilde{E}, \tilde{I}, \tilde{R}, \tilde{V}(t)) = (\tilde{S} - a - a\frac{\ln \tilde{S}}{a}) + (\tilde{E} - 1 - \ln \tilde{E}) + (\tilde{I} - 1 - \ln \tilde{I}) + (\tilde{R} - 1 - \ln \tilde{R}) + (\tilde{V} - 1 - \ln \tilde{V}) + \int_t^{t+\tau} a\Psi I(\tilde{s} - \tau)d\tilde{s}, \tag{4.3}$$

herein $a > 0$ be computed. We achieve, by applying Itô's formula,

$$d\mathbb{V} = \varsigma_1(\tilde{S} - a)dB_1(t) + \varsigma_2(\tilde{E} - 1)dB_2(t) + \varsigma_3(\tilde{I} - 1)dB_3(t) + \varsigma_4(\tilde{R} - 1)dB_4(t) + \varsigma_5(\tilde{V} - 1)dB_5(t) + L\mathbb{V}dt,$$

where

$$\begin{aligned} L\mathbb{V} =& (1 - \frac{a}{\tilde{S}})\left[(1 - \nu)\Lambda + \omega\tilde{R}(t) - \Psi\tilde{S}\,\tilde{I}(t - \tau) - \nu_r\tilde{S}(t) - d\tilde{S}(t) - \eta\tilde{S}(t) + \sigma\tilde{V}(t)\right] \\ &+ (1 - \frac{1}{\tilde{E}})\left[\Psi\tilde{S}(t)\tilde{I}(t - \tau) - (Q + d + l)\tilde{E}(t)\right] \\ &+ (1 - \frac{1}{\tilde{I}})\left[Q\tilde{E}(t) - (\kappa + d + l)\tilde{I}(t)\right] \\ &+ (1 - \frac{1}{\tilde{R}})\left[\Lambda\nu + \kappa\tilde{I}(t) - (d + \omega)\tilde{R}(t) + \nu_r\tilde{S}(t)\right] \\ &+ (1 - \frac{1}{\tilde{V}})\left[\eta\tilde{S}(t) - \sigma\tilde{V}(t) - d\tilde{V}(t)\right] \\ &+ \frac{a\varsigma_1^2 + \varsigma_2^2 + \varsigma_3^2 + \varsigma_4^2 + \varsigma_5^2}{2} + a\Psi I(t) - a\Psi\tilde{I}(t - \tau). \end{aligned} \tag{4.4}$$

Now, simplifying and using the condition $a\Psi - (d + l) = 0$, we obtain:

$$L\mathbb{V} \leq \Lambda + a\nu_r + d(a + 4) + Q + 2l + \kappa + \omega + \eta + \sigma + \frac{a\varsigma_1^2 + \varsigma_2^2 + \varsigma_3^2 + \varsigma_4^2 + \varsigma_5^2}{2} := \S, \tag{4.5}$$

here § > 0, which is independent from $\tilde{S}(t), \tilde{E}(t), \tilde{I}(t), \tilde{R}(t), \tilde{V}(t)$. Thus,

$$d\mathbb{V}(\tilde{S}, \tilde{E}, \tilde{I}, \tilde{R}, \tilde{V}) = \varsigma_1(\tilde{S}-a)dB_1(t)+\varsigma_2(\tilde{E}-1)dB_2(t)+\varsigma_3(\tilde{I}-1)dB_3(t)+\varsigma_4(\tilde{R}-1)dB_4(t)+\varsigma_5(\tilde{V}-1)dB_5(t)+\S dt. \tag{4.6}$$

By integrating of Eq (4.6) in 0 to $\tau_n \wedge \widetilde{\mathbb{T}} = \min\{\tau_n, \widetilde{\mathbb{T}}\}$, then on both sides, considering the expected value E, we can achieve

$$E\mathbb{V}\Big(\tilde{S}(\tau_k \wedge \widetilde{\mathbb{T}}), \tilde{I}(\tau_k \wedge \widetilde{\mathbb{T}}), \tilde{E}(\tau_k \wedge \widetilde{\mathbb{T}}), \tilde{R}(\tau_k \wedge \widetilde{\mathbb{T}}), \tilde{V}(\tau_k \wedge \widetilde{\mathbb{T}})\Big) \leq \S\widetilde{T} + E\mathbb{V}\Big(\tilde{S}(0), \tilde{I}(0), \tilde{E}(0), \tilde{R}(0), \tilde{V}(0)\Big). \tag{4.7}$$

Considering that $\Omega_k = \{\tau_k \leq \widetilde{\mathbb{T}}\}$, where $n \geq k_1$ according to Eq (4.2), it follows that $P(\Omega_k) \geq \epsilon$. This implies that for every $\varpi \in \Omega_k$, at least one of $\tilde{S}(\tau_k, \varpi), \tilde{E}(\tau_k, \varpi), \tilde{I}(\tau_k, \varpi), \tilde{R}(\tau_k, \varpi)$, or $\tilde{V}(\tau_k, \varpi)$ can be equal in terms of either $\frac{1}{k}$ or k, as follows

$$\mathbb{V}\Big(\tilde{S}(\tau_k \wedge \widetilde{\mathbb{T}}), \tilde{I}(\tau_k \wedge \widetilde{\mathbb{T}}, \tilde{E}(\tau_k \wedge \widetilde{\mathbb{T}})), \tilde{R}(\tau_k \wedge \widetilde{\mathbb{T}}), \tilde{V}(\tau_k \wedge \widetilde{\mathbb{T}})\Big) \geq (-\ln k + k - 1) \wedge \Big(-\ln\frac{1}{k} + \frac{1}{k} - 1\Big). \tag{4.8}$$

Through Eq (4.7), we get:

$$\begin{aligned} E\mathbb{V}(\tilde{S}(0), \tilde{I}(0), \bar{E}(0), \tilde{R}(0), \tilde{V}(0)) + \S\widetilde{T} &\geq E[1_{\Omega_k(\varpi)}\mathbb{V}\tilde{S}(\tau_k, \varpi), \tilde{E}(\tau_k, \varpi), \tilde{I}(\tau_k, \varpi), \tilde{R}(\tau_k, \varpi), \tilde{V}(\tau_k, \varpi)] \\ &\geq \epsilon(-\ln k + k - 1) \wedge \Big(-\ln\frac{1}{k} + \frac{1}{k} - 1\Big). \end{aligned} \tag{4.9}$$

Using an indicator operator 1_{Ω_k} to represent the indication of Ω_k, we can observe that as k approaches infinity, we have:

$$\infty > E\mathbb{V}(\tilde{S}(0), \tilde{E}(0), \tilde{I}(0), \tilde{R}(0), \tilde{V}(0)) + \S\widetilde{T} = \infty. \tag{4.10}$$

This observation challenges the initial assumption, leading us to $\tau_\infty = \infty$. This conclusion serves as proof for the desired outcome.

5. The existence of an ergodic stationary distribution

Here'in, a proper Lyapunov operator is created in the stochastic sense to deal with the positive root to the system (3.1) [35], such that there is one of a single ergodic stationary division. First, consider $\mathtt{Y}(t)$, which the stochastic differential equation in $\mathbb{R}^d$ has shown to be a regular time-homogeneous Markov process.

$$d\mathtt{Y}(t) = \sum_{m=1}^{d} \tilde{w}_m(t, \mathtt{Y}(t))dB_m(t) + \tilde{z}(\mathtt{Y}(t-\tau), \mathtt{Y}(t), t)dt. \tag{5.1}$$

The diffusion matrices for the process are,

$$\Delta(\mathtt{y}) = (\hbar_{ij}(\mathtt{y})), \quad \hbar_{ij}(\mathtt{y}) = \sum_{m=1}^{d} \tilde{w}_m^i(\mathtt{y})\tilde{w}_m^j(\mathtt{y}).$$

Lemma 5.1. *The Markov process $\Upsilon(t)$ possesses an ergodic stationary distributions $\pi(.)$ if a bounded set $U \subset \mathbb{R}^d$ exists with a continuous boundary Γ. Moreover,*

(i) For every $\mathsf{y} \in U, t \in \mathbb{R}^d, \exists K > 0$ such that $\sum_{i,j=1}^{d} \hbar_{ij}(\mathsf{y})\zeta_i\zeta_j \geq K|\zeta|^2$.
(ii) $\forall \mathbb{R}^d \backslash U$, exists a positive C^2 operator such that $\widetilde{\mathbb{V}}$; $L\widetilde{\mathbb{V}} < 0$.

Consider the stochastic approach's fundamental model reproduction number as follows:

$$R_0^s = \frac{\Lambda(1-\eta)\psi Q}{\hat{\mu}\hat{\epsilon}\hat{\alpha}\hat{\gamma}}, \tag{5.2}$$

where

$$\hat{\mu} = d + \nu_r + \eta + \frac{\varsigma_1^2}{2}, \quad \hat{\epsilon} = d + Q + l + \frac{\varsigma_2^2}{2}, \quad \hat{\alpha} = \kappa + d + l + \frac{\varsigma_3^2}{2}, \quad \hat{\gamma} = d + \omega + \frac{\varsigma_4^2}{2}, \quad \hat{\sigma} = d + \sigma + \frac{\varsigma_5^2}{2}.$$

Theorem 5.2. *Let $R_0^s > 1$ for all cases $d - \frac{\varsigma_1^2 \vee \varsigma_2^2 \vee \varsigma_3^2 \vee \varsigma_4^2 \vee \varsigma_5^2}{2} > 0$. Subsequently, for $(\tilde{S}(0), \tilde{E}(0), \tilde{I}(0), \tilde{R}(0), \tilde{V}(0)) \in \mathbb{R}_+^5$, there is one ergodic stationary division $\pi(.)$ of the system given by the model (3.1).*

Proof. As a first step to prove the theorem, we check the conditions of Lemma 1 are satisfied. In order to arrive at the outcome of (i), the diffusion matrix of the system given by model (3.1) is given as

$$\Delta = \begin{pmatrix} \varsigma_1^2\tilde{S}^2 & 0 & 0 & 0 & 0 \\ 0 & \varsigma_2^2\tilde{E}^2 & 0 & 0 & 0 \\ 0 & 0 & \varsigma_3^2\tilde{I}^2 & 0 & 0 \\ 0 & 0 & 0 & \varsigma_4^2\tilde{R}^2 & 0 \\ 0 & 0 & 0 & 0 & \varsigma_5^2\tilde{V}^2 \end{pmatrix}. \tag{5.3}$$

Criterion (i) of Lemma 1 obeys, is positively definite at any of the compact subsets of $\mathbb{R}_+^5$.
We now check Criterion (ii). We consider C^2-operator $\mathbb{V} : \mathbb{R}_+^5 \to \mathbb{R}$ in the underling as follows:

$$\begin{aligned} \mathbb{V}(\tilde{S}, \tilde{E}, \tilde{I}, \tilde{R}, \tilde{V}) =& c_1\Psi \int_t^{t+\tau} \tilde{I}(\tilde{s}-\tau)d\tilde{s} + N\Big(c_1\Psi \int_t^{t+\tau} \tilde{I}(\tilde{s}-\tau)d\tilde{s} - \ln\tilde{S}\, c_1 - c_3 \ln\tilde{I} - c_2 \ln\tilde{E} \\ & - \ln\tilde{R} - \ln\tilde{V}\Big) \\ & - \ln\tilde{S} - \ln\tilde{R} - \ln\tilde{V} - \ln\tilde{E} + \frac{1}{\varrho+1}(\tilde{S} + \tilde{E} + \tilde{I} + \tilde{R} + \tilde{V})^{\varrho+1} \\ =& N\mathbb{V}_1 + \mathbb{V}_2 + \mathbb{V}_3 + \mathbb{V}_4 + \mathbb{V}_5 + \mathbb{V}_6, \end{aligned} \tag{5.4}$$

where

$$\mathsf{c}_1 = \frac{\Lambda\Psi Q}{\hat{u}^2\hat{\epsilon}\hat{\alpha}} + \frac{\eta}{\hat{u}}, \quad \mathsf{c}_2 = \frac{\Lambda\Psi Q}{\hat{u}\hat{\epsilon}^2\hat{\alpha}} + \frac{\sigma}{\hat{\epsilon}}, \quad \mathsf{c}_3 = \frac{\Lambda\Psi Q}{\hat{u}\hat{\epsilon}\hat{\alpha}^2}.$$

Note that $\mathtt{V}(\tilde{S}, \tilde{E}, \tilde{I}, \tilde{R})$ is defined not only on every single point.However it also reaches $+\infty$ as $(\tilde{S}, \tilde{E}, \tilde{I}, \tilde{R}, \tilde{V})$ is limited to $\mathbb{R}_+^5$ also $\|(\tilde{S}, \tilde{E}, \tilde{I}, \tilde{R}, \tilde{V})\| \to \infty$. Due to this, we achieve a minor point,

$(\tilde{S}(0), \tilde{E}(0), \tilde{I}(0), \tilde{R}(0), \tilde{V}(0))$ within domain of $\mathbb{R}^5_+$. We also take C^2- the operator $\tilde{\mathbb{V}} : \mathbb{R}^5_+ \to \mathbb{R}_+$ in the following way:

$$\begin{aligned}\widetilde{\mathbb{V}}(\tilde{S}, \tilde{E}, \tilde{I}, \tilde{R}, \tilde{V}) &= \mathsf{c}_1\Psi \int_t^{t+\tau} \tilde{I}(-\tau + \tilde{s})d\tilde{s} \\ &+ N\Big(- \ln \tilde{R} - \ln \tilde{V} - \ln \tilde{S}\,\mathsf{c}_1 - \mathsf{c}_3 \ln \tilde{I} - \mathsf{c}_2 \ln \tilde{E} + \mathsf{c}_1\Psi \int_t^{t+\tau} \tilde{I}(-\tau + \tilde{s})d\tilde{s}\Big) - \ln \tilde{S} \\ &- \ln \tilde{R} - \ln \tilde{V} - \ln \tilde{E} + \frac{1}{\varrho + 1}(\tilde{S} + \tilde{I} + \tilde{E} + \tilde{R} + \tilde{V})^{\varrho+1} \\ &- \mathbb{V}(\tilde{S}(0), \tilde{I}(0), \tilde{E}(0), \tilde{R}(0), \tilde{V}(0)) \\ &:= -\mathbb{V}(\tilde{S}(0), \tilde{I}(0), \tilde{E}(0), \tilde{R}(0), \tilde{V}(0)) + N\mathbb{V}_1 + \mathbb{V}_2 + \mathbb{V}_3 + \mathbb{V}_4 + \mathbb{V}_5 + \mathbb{V}_6.\end{aligned} \tag{5.5}$$

Here $(\tilde{S}, \tilde{E}, \tilde{I}, \tilde{R}) \in (\frac{1}{k}, k) \times (\frac{1}{k}, k) \times (\frac{1}{k}, k) \times (\frac{1}{k}, k)$ and $k > 1$ is a so larger integer,

$$\begin{aligned}\mathbb{V}_1 &= c_1\Psi \int_t^{t+\tau} \tilde{I}(\tilde{s} - \tau)d\tilde{s} - \mathsf{c}_1 \ln \tilde{S} - \mathsf{c}_2 \ln \tilde{E} - \ln \tilde{R} - \ln \tilde{V} - \mathsf{c}_3 \ln \tilde{I}, \\ \mathbb{V}_2 &= c_1\Psi \int_t^{t+\tau} \tilde{I}(\tilde{s} - \tau)d\tilde{s} - \ln \tilde{S}, \\ \mathbb{V}_3 &= -\ln \tilde{E}, \quad \mathbb{V}_4 = -\ln \tilde{R}, \quad \mathbb{V}_5 = -\ln \tilde{V}, \\ \mathbb{V}_6 &= \frac{1}{\varrho + 1}(\tilde{S} + \tilde{E} + \tilde{I} + \tilde{R} + \tilde{V})^{\varrho+1},\end{aligned}$$

$\varrho > 1$, fulfilling $d - \frac{\varrho}{2}(\varsigma_1^2 \vee \varsigma_2^2 \vee \varsigma_3^2 \vee \varsigma_4^2) > 0$. The value of $N > 0$ is also much larger, obeying the result $-N\delta + \mathsf{R} \le -2$, and in this, we have $\delta = \frac{\Lambda\psi Q}{\hat{\mu}\hat{\epsilon}\hat{\alpha}} - (d + \omega + \frac{\varsigma_4^2}{2}) > 0$

$$\begin{aligned}\mathsf{R} = \sup_{(\tilde{S},\tilde{E},\tilde{I},\tilde{R},\tilde{V})\in\mathbb{R}^5_+} \Big(&- \frac{1}{4}\Big[d - \frac{\varrho}{2}(\varsigma_1^2 \vee \varsigma_2^2 \vee \varsigma_3^2 \vee \varsigma_4^2 \vee \varsigma_5^2)\Big]\tilde{I}^{\varrho+1} \\ &+ \nu_r + 2d + Q + l + \omega + \mathsf{B} + \frac{\varsigma_1^2}{2} + \frac{\varsigma_2^2}{2} + \frac{\varsigma_3^2}{2} + \eta + \sigma + \frac{\varsigma_5^2}{2}\Big),\end{aligned} \tag{5.6}$$

and

$$\begin{aligned}B =: \sup_{(\tilde{S},\tilde{E},\tilde{I},\tilde{R},\tilde{V})\in\mathbb{R}^5_+} \Big\{ &\Lambda(\tilde{S} + \tilde{E} + \tilde{I} + \tilde{R} + \tilde{V})^{\varrho} - \frac{1}{2}\Big[d - \frac{\varrho}{2}(\varsigma_1^2 \vee \varsigma_2^2 \vee \varsigma_3^2 \vee \varsigma_4^2 \vee \varsigma_5^2)\Big] \\ &\times (\tilde{S} + \tilde{E} + \tilde{I} + \tilde{R} + \tilde{V})^{\varrho+1}\Big\} < \infty.\end{aligned} \tag{5.7}$$

By applying Itô's formula to $\mathbb{V}_1$, we get:

$$\begin{aligned} L\mathbb{V}_1 &= -\frac{c_1\Lambda}{\tilde{S}} + c_1\nu_r + c_1 d + \frac{c_1\varsigma_1^2}{2} - \frac{c_2\Psi\tilde{S}\tilde{I}}{\tilde{E}} + c_2(Q+d+l) + \frac{c_2\varsigma_2^2}{2} \\ &\quad - \frac{c_3 Q\tilde{E}}{\tilde{I}} + c_3(\kappa+d+l) + \frac{c_3\varsigma_3^2}{2} - \frac{\kappa\tilde{I}}{\tilde{R}} + (d+\omega) + \frac{\varsigma_4^2}{2} + c_1\Psi\tilde{I}(t) \\ &\quad - c_1\eta + c_5\sigma\tilde{V} \\ &\leq -3\sqrt[3]{\Lambda\Psi Q c_1 c_2 c_3} + c_1\left(\nu_r + d + \frac{\varsigma_1^2}{2} - \eta\right) + c_2\left(Q + d + l + \frac{\varsigma_2^2}{2}\right) \\ &\quad + c_3\left(\kappa + d + l + \frac{\varsigma_3^2}{2}\right) + \left(d + \omega + \frac{\varsigma_4^2}{2}\right) + c_1\Psi\tilde{I}(t) + c_5\sigma\tilde{V} \\ &\leq \frac{\Lambda\psi Q}{\hat{\mu}\hat{\epsilon}\hat{\alpha}} + \left(d + \omega + \frac{\varsigma_4^2}{2}\right) + c_1\psi\tilde{I}(t) - c_1\eta + c_5\sigma\tilde{V} \\ &= -\delta + c_1\psi\tilde{I}(t) - c_1\eta + c_5\sigma\tilde{V}. \end{aligned} \tag{5.8}$$

Similarly, we obtain:

$$L\mathbb{V}_2 = -\frac{\Lambda}{\tilde{S}} + \nu_r + \frac{\Lambda\nu}{\tilde{S}} - \frac{\omega\tilde{R}}{\tilde{S}} + \mathsf{c}_1\psi\tilde{I} + \frac{\varsigma_1^2}{2} - \frac{\eta\tilde{S}}{\tilde{S}} + \frac{\sigma\tilde{V}}{\tilde{S}}, \tag{5.9}$$

$$L\mathbb{V}_3 = -\frac{\psi\tilde{S}\tilde{I}(t-\tau)}{\tilde{E}} + (d+Q+l) + \frac{\varsigma_2^2}{2}, \tag{5.10}$$

$$L\mathbb{V}_4 = -\frac{\Lambda\nu}{\tilde{R}} - \frac{\kappa\tilde{I}}{\tilde{R}} - \frac{\nu_r\tilde{S}}{\tilde{R}} + (d+\omega) + \frac{\varsigma_4^2}{2} + \frac{\eta\tilde{S}}{\tilde{R}} - \frac{\sigma\tilde{V}}{\tilde{R}}, \tag{5.11}$$

$$L\mathbb{V}_5 = -\frac{\eta\tilde{S}}{\tilde{V}} + \sigma + d, \tag{5.12}$$

$$\begin{aligned} L\mathbb{V}_6 &= (\tilde{S}+\tilde{E}+\tilde{I}+\tilde{R}+\tilde{V})^{\varrho}[\Lambda - d(\tilde{S}+\tilde{E}+\tilde{I}+\tilde{R}+\tilde{V}) - l\tilde{E} - l\tilde{I} - l\tilde{V} - \sigma\tilde{V} + \eta\tilde{S}] \\ &\quad + \frac{\varrho}{2}(\tilde{S}+\tilde{E}+\tilde{I}+\tilde{R}+\tilde{V})^{\varrho-1}(\varsigma_1^2\tilde{S}^2 \vee \varsigma_2^2\tilde{E}^2 \vee \varsigma_3^2\tilde{I}^2 \vee \varsigma_4^2\tilde{R}^2 \vee \varsigma_5^2\tilde{V}^2) \\ &\leq -(\tilde{S}+\tilde{E}+\tilde{I}+\tilde{R}+\tilde{V})^{\varrho+1}\left[d - \frac{\varrho}{2}(\varsigma_1^2 \vee \varsigma_2^2 \vee \varsigma_3^2 \vee \varsigma_4^2 \vee \varsigma_5^2)\right] + \Lambda(\tilde{S}+\tilde{E}+\tilde{I}+\tilde{R}+\tilde{V})^{\varrho} \\ &\leq -\frac{1}{2}\left[d - \frac{\varrho}{2}(\varsigma_1^2 \vee \varsigma_2^2 \vee \varsigma_3^2 \vee \varsigma_4^2 \vee \varsigma_5^2)\right](\tilde{S}^{\rho+1} + \tilde{E}^{\varrho+1} + \tilde{I}^{\varrho+1} + \tilde{R}^{\varrho+1} + \tilde{V}^{\varrho+1}) + B. \end{aligned} \tag{5.13}$$

B is given in Eq (5.7). From Eq (5.13), we get the following:

$$\begin{aligned} L\widetilde{\mathbb{V}} &\leq -N\delta + N\mathsf{c}_1\Psi\tilde{I} - \frac{1}{2}\Big[d - \frac{\varrho}{2}(\varsigma_1^2 \vee \varsigma_2^2 \vee \varsigma_3^2 \vee \varsigma_4^2 \vee \varsigma_5^2)\Big] \\ &\quad \times (\tilde{S}^{\varrho+1} + \tilde{E}^{\varrho+1} + \tilde{I}^{\varrho+1} + \tilde{R}^{\varrho+1} + \tilde{V}^{\varrho+1}) \\ &\quad + \nu_r + 2d + Q + l + \omega - \frac{\Lambda}{\tilde{S}} - \frac{\omega\tilde{R}}{\tilde{S}} + \mathsf{c}_1\Psi\tilde{I} - \frac{\Lambda\nu}{\tilde{R}} - \frac{\kappa\tilde{I}}{\tilde{R}} - \frac{\nu_r\tilde{S}}{\tilde{R}} \\ &\quad + B + \frac{\varsigma_1^2}{2} + \frac{\varsigma_2^2}{2} + \frac{\varsigma_4^2}{2} + \frac{\varsigma_5^2}{2} - \frac{\gamma\tilde{V}}{\tilde{S}} + \gamma - \frac{\Lambda}{\tilde{V}} \\ &\leq -N\delta + N\mathsf{c}_1\Psi\tilde{I} - \frac{1}{4}\Big[d - \frac{\varrho}{2}(\varsigma_1^2 \vee \varsigma_2^2 \vee \varsigma_3^2 \vee \varsigma_4^2 \vee \varsigma_5^2)\Big] \\ &\quad \times (\tilde{S}^{\varrho+1} + \tilde{E}^{\varrho+1} + \tilde{I}^{\varrho+1} + \tilde{R}^{\varrho+1} + \tilde{V}^{\varrho+1}) \\ &\quad + \nu_r + 2d + Q + L + \omega - \frac{\Lambda}{\tilde{S}} - \frac{1}{4}\Big[d - \frac{\varrho}{2}(\varsigma_1^2 \vee \varsigma_2^2 \vee \varsigma_3^2 \vee \varsigma_4^2 \vee \varsigma_5^2)\Big]I^{\varrho+1} \\ &\quad - \frac{\kappa I}{R} + \Psi\tilde{I} - \frac{\nu_r\tilde{S}}{\tilde{R}} - \frac{\omega\tilde{R}}{\tilde{S}} + B + \frac{\varsigma_1^2}{2} + \frac{\varsigma_2^2}{2} + \frac{\varsigma_4^2}{2} + \frac{\varsigma_5^2}{2} - \frac{\gamma\tilde{V}}{\tilde{S}} + \gamma. \end{aligned} \tag{5.14}$$

For $\chi > 0$, we define a closed bounded set as follows:

$$\mathbb{F} = \left\{(\tilde{S}, \tilde{E}, \tilde{I}, \tilde{R}, \tilde{V}) \in \mathbb{R}_+^5 : \chi \leq \tilde{S} \leq \frac{1}{\chi}, \chi_1 \leq \tilde{E} \leq \frac{1}{\chi_1}, \chi_2 \leq \tilde{I} \leq \frac{1}{\chi_2}, \chi_3 \leq \tilde{R} \leq \frac{1}{\chi_3}, \chi_4 \leq \tilde{V} \leq \frac{1}{\chi_4}\right\}. \tag{5.15}$$

Consider the criteria in $\mathbb{R}_+^5 \backslash \mathbb{F}$, as follows

$$-\frac{\Lambda}{\chi} + \mathbb{J} \leq -1, \tag{5.16}$$

$$-\frac{1}{4}\Big[d - \frac{\varrho}{2}(\varsigma_1^2 \vee \varsigma_2^2 \vee \varsigma_3^2 \vee \varsigma_4^2 \vee \varsigma_5^2)\Big]\chi^{\varrho+1} + \mathbb{J} \leq -1, \tag{5.17}$$

$$-\frac{\kappa\chi_2}{\chi_3} - \frac{\lambda\chi_5}{\chi_1} + Nc_1\psi\chi_2 + \mathtt{R} \leq -1, \tag{5.18}$$

$$-\frac{\lambda\chi_5}{\chi_1} + \mathbb{J} \leq -1, \tag{5.19}$$

$$-\frac{1}{4}\Big[d - \frac{\varrho}{2}(\varsigma_1^2 \vee \varsigma_2^2 \vee \varsigma_3^2 \vee \varsigma_4^2 \vee \varsigma_5^2)\Big]\frac{1}{\chi^{\varrho+1}} + \mathbb{J} \leq -1, \tag{5.20}$$

$$-\frac{1}{4}\Big[d - \frac{\varrho}{2}(\varsigma_1^2 \vee \varsigma_2^2 \vee \varsigma_3^2 \vee \varsigma_4^2 \vee \varsigma_5^2)\Big]\frac{1}{\chi_1^{\varrho+1}} + \mathbb{J} \leq -1, \tag{5.21}$$

$$-\frac{1}{4}\Big[d - \frac{\varrho}{2}(\varsigma_1^2 \vee \varsigma_2^2 \vee \varsigma_3^2 \vee \varsigma_4^2 \vee \varsigma_5^2)\Big]\frac{1}{\chi_2^{\varrho+1}} + \mathbb{J} \leq -1, \tag{5.22}$$

$$-\frac{1}{4}\Big[d - \frac{\varrho}{2}(\varsigma_1^2 \vee \varsigma_2^2 \vee \varsigma_3^2 \vee \varsigma_4^2 \vee \varsigma_5^2)\Big]\frac{1}{\chi_3^{\varrho+1}} + \mathbb{J} \leq -1, \tag{5.23}$$

$$-\frac{1}{4}\Big[d - \frac{\varrho}{2}(\varsigma_1^2 \vee \varsigma_2^2 \vee \varsigma_3^2 \vee \varsigma_4^2 \vee \varsigma_5^2)\Big]\frac{1}{\chi_4^{\varrho+1}} + \mathbb{J} \leq -1, \tag{5.24}$$

where

$$\begin{aligned}\mathbb{J} = \sup_{(\tilde{S},\tilde{E},\tilde{I},\tilde{R},\tilde{V})\in\mathbb{R}^5_+} &\Big\{Nc_1\psi\tilde{I} - \frac{1}{4}\Big[d - \frac{\varrho}{2}(\varsigma_1^2 \vee \varsigma_2^2 \vee \varsigma_3^2 \vee \varsigma_4^2 \vee \varsigma_5^2)\Big]I^{\varrho+1} \\ &+ \nu_r + 2d + Q + l + \omega + \mathtt{B} + \frac{\varsigma_1^2}{2} + \frac{\varsigma_2^2}{2} + \frac{\varsigma_4^2}{2} + \frac{\varsigma_5^2}{2}\Big\}.\end{aligned} \tag{5.25}$$

For the new model, we redefine the sets $\mathbb{F}_i$ on the basis of the modified system. Assuming the new model includes five compartments $(\tilde{S}, \tilde{E}, \tilde{I}, \tilde{R}, \tilde{V})$, we have

$$\mathbb{R}^5_+ \backslash \mathbb{F} = \bigcup_{i=1}^{10} \mathbb{F}_i,$$

where

$$\begin{aligned}
\mathbb{F}_1 &= \Big\{(\tilde{S}, \tilde{E}, \tilde{I}, \tilde{R}, \tilde{V}) \in \mathbb{R}^5_+; 0 < \tilde{S} < \chi\Big\}, \\
\mathbb{F}_2 &= \Big\{(\tilde{S}, \tilde{E}, \tilde{I}, \tilde{R}, \tilde{V}) \in \mathbb{R}^5_+; 0 < \tilde{E} < \chi_1\Big\}, \\
\mathbb{F}_3 &= \Big\{(\tilde{S}, \tilde{E}, \tilde{I}, \tilde{R}, \tilde{V}) \in \mathbb{R}^5_+; 0 < \tilde{I} < \chi_2, \tilde{E} \geq \chi_1\Big\}, \\
\mathbb{F}_4 &= \Big\{(\tilde{S}, \tilde{E}, \tilde{I}, \tilde{R}, \tilde{V}) \in \mathbb{R}^5_+; 0 < \tilde{R} < \chi_3, \tilde{I} \geq \chi_2\Big\}, \\
\mathbb{F}_5 &= \Big\{(\tilde{S}, \tilde{E}, \tilde{I}, \tilde{R}, \tilde{V}) \in \mathbb{R}^5_+; 0 < \tilde{V} < \chi_4, \tilde{R} \geq \chi_3\Big\}, \\
\mathbb{F}_6 &= \Big\{(\tilde{S}, \tilde{E}, \tilde{I}, \tilde{R}, \tilde{V}) \in \mathbb{R}^5_+; \tilde{S} > \frac{1}{\chi}\Big\}, \\
\mathbb{F}_7 &= \Big\{(\tilde{S}, \tilde{E}, \tilde{I}, \tilde{R}, \tilde{V}) \in \mathbb{R}^5_+; \tilde{E} > \frac{1}{\chi_1}\Big\}, \\
\mathbb{F}_8 &= \Big\{(\tilde{S}, \tilde{E}, \tilde{I}, \tilde{R}, \tilde{V}) \in \mathbb{R}^5_+; \tilde{I} > \frac{1}{\chi_2}\Big\}, \\
\mathbb{F}_9 &= \Big\{(\tilde{S}, \tilde{E}, \tilde{I}, \tilde{R}, \tilde{V}) \in \mathbb{R}^5_+; \tilde{R} > \frac{1}{\chi_3}\Big\}, \\
\mathbb{F}_{10} &= \Big\{(\tilde{S}, \tilde{E}, \tilde{I}, \tilde{R}, \tilde{V}) \in \mathbb{R}^5_+; \tilde{V} > \frac{1}{\chi_4}\Big\}.
\end{aligned} \tag{5.26}$$

Case 1. For each $(\tilde{S}, \tilde{E}, \tilde{I}, \tilde{R}, \tilde{V}) \in \mathbb{F}_1$, we achieve:

$$\begin{aligned}
L\widetilde{\mathbb{V}} &\leq -\frac{\Lambda}{\tilde{S}} + Nc_1\psi\tilde{I} + Nc_2\psi\tilde{V} - \frac{1}{4}\Big[d - \frac{\varrho}{2}(\varsigma_1^2 \vee \varsigma_2^2 \vee \varsigma_3^2 \vee \varsigma_4^2 \vee \varsigma_5^2)\Big]\tilde{I}^{\varrho+1} \\
&\quad + \nu_r + 2d + Q + l + \omega + B + \frac{\varsigma_2^2}{2} + \frac{\varsigma_1^2}{2} + \frac{\varsigma_4^2}{2} + \frac{\varsigma_5^2}{2} \\
&\leq -\frac{\Lambda}{\tilde{S}} + \mathbb{J} \\
&\leq -\frac{\Lambda}{\chi} + \mathbb{J} \leq -1.
\end{aligned} \tag{5.27}$$

This can be found in Eq (5.16). Thus, $L\widetilde{\mathbb{V}} \leq -1$ for each $(\tilde{S}, \tilde{E}, \tilde{I}, \tilde{R}, \tilde{V}) \in \mathbb{F}_1$.
Case 2. For each $(\tilde{S}, \tilde{E}, \tilde{I}, \tilde{R}, \tilde{V}) \in \mathbb{F}_2$ yields the following

$$\begin{aligned} L\widetilde{\mathbb{V}} \leq\ & N\mathsf{c}_1\psi\tilde{I} - \frac{1}{4}\Big[d - \frac{\varrho}{2}(\varsigma_1^2 \vee \varsigma_2^2 \vee \varsigma_3^2 \vee \varsigma_4^2 \vee \varsigma_5^2)\Big]\tilde{E}^{\varrho+1} \\ & - \frac{1}{4}\Big[d - \frac{\varrho}{2}(\varsigma_1^2 \vee \varsigma_2^2 \vee \varsigma_3^2 \vee \varsigma_4^2 \vee \varsigma_5^2)\Big]\tilde{I}^{\varrho+1} \\ & + \nu_r + 2d + Q + l + \omega + B + \frac{\varsigma_2^2}{2} + \frac{\varsigma_1^2}{2} + \frac{\varsigma_4^2}{2} + \frac{\varsigma_5^2}{2} \\ \leq\ & -\frac{1}{4}\Big[d - \frac{\varrho}{2}(\varsigma_1^2 \vee \varsigma_2^2 \vee \varsigma_3^2 \vee \varsigma_4^2 \vee \varsigma_5^2)\Big]\chi_1^{\varrho+1} + \mathbb{J} \leq -1. \end{aligned} \tag{5.28}$$

This can be found in Eq (5.17). As a result, $L\widetilde{\mathbb{V}} \leq -1$ for each $(\tilde{S}, \tilde{E}, \tilde{I}, \tilde{R}, \tilde{V}) \in \mathbb{F}_2$.
Case 3. For each $(\tilde{S}, \tilde{E}, \tilde{I}, \tilde{R}, \tilde{V}) \in \mathbb{F}_3$, we obtain:

$$\begin{aligned} L\widetilde{\mathbb{V}} \leq\ & -\frac{\kappa\tilde{I}}{\tilde{R}} - \frac{\lambda\tilde{V}}{\tilde{S}} + Nc_1\psi\tilde{I} \\ & - \frac{1}{4}\Big[d - \frac{\varrho}{2}(\varsigma_1^2 \vee \varsigma_2^2 \vee \varsigma_3^2 \vee \varsigma_4^2 \vee \varsigma_5^2)\Big]\tilde{I}^{\varrho+1} \\ & - \frac{1}{4}\Big[d - \frac{\varrho}{2}(\varsigma_1^2 \vee \varsigma_2^2 \vee \varsigma_3^2 \vee \varsigma_4^2 \vee \varsigma_5^2)\Big]\tilde{V}^{\varrho+1} \\ & + \nu_r + 2d + Q + l + \omega + B + \frac{\varsigma_2^2}{2} + \frac{\varsigma_1^2}{2} + \frac{\varsigma_4^2}{2} + \frac{\varsigma_5^2}{2} \\ \leq\ & -\frac{\kappa\tilde{I}}{\tilde{R}} - \frac{\lambda\tilde{V}}{\tilde{S}} + Nc_1\psi\tilde{I} + \mathrm{R} \\ \leq\ & -\frac{\kappa\chi_2}{\chi_3} - \frac{\lambda\chi_5}{\chi_1} + Nc_1\psi\chi_2 + \mathrm{R} \leq -1. \end{aligned} \tag{5.29}$$

This can be found in Eq (5.18). As a result, $L\widetilde{\mathbb{V}} \leq -1$ at each $(\tilde{S}, \tilde{E}, \tilde{I}, \tilde{R}, \tilde{V}) \in \mathbb{F}_3$.
Case 4. For each $(\tilde{S}, \tilde{E}, \tilde{I}, \tilde{R}, \tilde{V}) \in \mathbb{F}_4$, we obtain:

$$\begin{aligned} L\widetilde{\mathbb{V}} \leq\ & -\frac{\kappa\tilde{I}}{\tilde{R}} - \frac{\lambda\tilde{V}}{\tilde{S}} + N\mathsf{c}_1\beta\tilde{I} \\ & - \frac{1}{4}\Big[d - \frac{\varrho}{2}(\varsigma_1^2 \vee \varsigma_2^2 \vee \varsigma_3^2 \vee \varsigma_4^2 \vee \varsigma_5^2)\Big]\tilde{I}^{\varrho+1} \\ & + \nu_r + 2d + Q + l + \omega + B + \frac{\varsigma_2^2}{2} + \frac{\varsigma_1^2}{2} + \frac{\varsigma_4^2}{2} + \frac{\varsigma_5^2}{2} \\ \leq\ & -\frac{\kappa\tilde{I}}{\tilde{R}} - \frac{\lambda\tilde{V}}{\tilde{S}} + \mathbb{J} \\ \leq\ & -\frac{\kappa\chi_2}{\chi_3} - \frac{\lambda\chi_5}{\chi_1} + \mathbb{J} \leq -1. \end{aligned} \tag{5.30}$$

This can be found in Eq (5.18). As a result, $L\widetilde{\mathbb{V}} \leq -1$ at each $(\tilde{S}, \tilde{E}, \tilde{I}, \tilde{R}, \tilde{V}) \in \mathbb{F}_4$.

Case 5. For each $(\tilde{S}, \tilde{E}, \tilde{I}, \tilde{R}, \tilde{V}) \in \mathbb{F}_5$, we obtain:

$$\begin{aligned} L\widetilde{\mathbb{V}} \leq & -\frac{\lambda\tilde{V}}{\tilde{S}} + N\mathsf{c}_1\beta\tilde{I} \\ & - \frac{1}{4}\Big[d - \frac{\varrho}{2}(\varsigma_1^2 \vee \varsigma_2^2 \vee \varsigma_3^2 \vee \varsigma_4^2 \vee \varsigma_5^2)\Big]\tilde{I}^{\varrho+1} \\ & + \nu_r + 2d + Q + l + \omega + B + \frac{\varsigma_2^2}{2} + \frac{\varsigma_1^2}{2} + \frac{\varsigma_4^2}{2} + \frac{\varsigma_5^2}{2} \\ \leq & -\frac{\lambda\tilde{V}}{\tilde{S}} + \mathbb{J} \\ \leq & -\frac{\lambda\chi_5}{\chi_1} + \mathbb{J} \leq -1. \end{aligned} \tag{5.31}$$

This can be found in Eq (5.19). As a result, $L\widetilde{\mathbb{V}} \leq -1$ at each $(\tilde{S}, \tilde{E}, \tilde{I}, \tilde{R}, \tilde{V}) \in \mathbb{F}_5$.
Case 6. For each $(\tilde{S}, \tilde{E}, \tilde{I}, \tilde{R}, \tilde{V}) \in \mathbb{F}_6$, we obtain:

$$\begin{aligned} L\widetilde{\mathbb{V}} \leq & -\frac{1}{4}\Big[d - \frac{\varrho}{2}(\varsigma_1^2 \vee \varsigma_2^2 \vee \varsigma_3^2 \vee \varsigma_4^2 \vee \varsigma_5^2)\Big]\tilde{S}^{\varrho+1} + N\mathsf{c}_1\Psi\tilde{I} \\ & - \frac{1}{4}\Big[d - \frac{\varrho}{2}(\varsigma_1^2 \vee \varsigma_2^2 \vee \varsigma_3^2 \vee \varsigma_4^2 \vee \varsigma_5^2)\Big]\tilde{I}^{\varrho+1} \\ & + \nu_r + 2d + Q + l + \omega + B + \frac{\varsigma_2^2}{2} + \frac{\varsigma_1^2}{2} + \frac{\varsigma_4^2}{2} + \frac{\varsigma_5^2}{2} \\ \leq & -\frac{1}{4}\Big[d - \frac{\varrho}{2}(\varsigma_1^2 \vee \varsigma_2^2 \vee \varsigma_3^2 \vee \varsigma_4^2 \vee \varsigma_5^2)\Big]\tilde{S}^{\varrho+1} + \mathbb{J} \\ \leq & -\frac{1}{4}\Big[d - \frac{\varrho}{2}(\varsigma_1^2 \vee \varsigma_2^2 \vee \varsigma_3^2 \vee \varsigma_4^2 \vee \varsigma_5^2)\Big]\frac{1}{\chi^{\varrho+1}} + \mathbb{J} \leq -1. \end{aligned} \tag{5.32}$$

This can be found in Eq (5.20). Thus, $L\widetilde{\mathbb{V}} \leq -1$ at each $(\tilde{S}, \tilde{E}, \tilde{I}, \tilde{R}, \tilde{V}) \in \mathbb{F}_6$.
Case 7. For each $(\tilde{S}, \tilde{E}, \tilde{I}, \tilde{R}, \tilde{V}) \in \mathbb{F}_7$,, we obtain:

$$\begin{aligned} L\widetilde{\mathbb{V}} \leq & -\frac{1}{4}\Big[d - \frac{\varrho}{2}(\varsigma_1^2 \vee \varsigma_2^2 \vee \varsigma_3^2 \vee \varsigma_4^2 \vee \varsigma_5^2)\Big]\tilde{E}^{\varrho+1} + N\mathsf{c}_1\psi\tilde{I} \\ & - \frac{1}{4}\Big[d - \frac{\varrho}{2}(\varsigma_1^2 \vee \varsigma_2^2 \vee \varsigma_3^2 \vee \varsigma_4^2 \vee \varsigma_5^2)\Big]\tilde{I}^{\varrho+1} \\ & + \nu_r + 2d + Q + l + \omega + B + \frac{\varsigma_2^2}{2} + \frac{\varsigma_1^2}{2} + \frac{\varsigma_4^2}{2} + \frac{\varsigma_5^2}{2} \end{aligned} \tag{5.33}$$

$$\begin{aligned} & \leq -\frac{1}{4}\Big[d - \frac{\varrho}{2}(\varsigma_1^2 \vee \varsigma_2^2 \vee \varsigma_3^2 \vee \varsigma_4^2 \vee \varsigma_5^2)\Big]\tilde{E}^{\varrho+1} + \mathbb{J} \\ & \leq -\frac{1}{4}\Big[d - \frac{\varrho}{2}(\varsigma_1^2 \vee \varsigma_2^2 \vee \varsigma_3^2 \vee \varsigma_4^2 \vee \varsigma_5^2)\Big]\frac{1}{\chi_1^{\varrho+1}} + \mathbb{J} \leq -1. \end{aligned} \tag{5.34}$$

This can be found in Eq (5.21). As a result, $L\widetilde{\mathbb{V}} \leq -1$ at each $(\tilde{S}, \tilde{E}, \tilde{I}, \tilde{R}, \tilde{V}) \in \mathbb{F}_7$.

Case 8. For each $(\tilde{S}, \tilde{E}, \tilde{I}, \tilde{R}, \tilde{V}) \in \mathbb{F}_8$, we obtain:

$$\begin{aligned} L\widetilde{\mathbb{V}} \leq N\mathsf{c}_1\beta\tilde{I} &- \frac{1}{4}\Big[d - \frac{\varrho}{2}(\varsigma_1^2 \vee \varsigma_2^2 \vee \varsigma_3^2 \vee \varsigma_4^2 \vee \varsigma_5^2)\Big]\tilde{I}^{\varrho+1} \\ &- \frac{1}{4}\Big[d - \frac{\varrho}{2}(\varsigma_1^2 \vee \varsigma_2^2 \vee \varsigma_3^2 \vee \varsigma_4^2 \vee \varsigma_5^2)\Big]\tilde{I}^{\varrho+1} \\ &+ \nu_r + 2d + Q + l + \omega + B + \frac{\varsigma_2^2}{2} + \frac{\varsigma_1^2}{2} + \frac{\varsigma_4^2}{2} + \frac{\varsigma_5^2}{2} \end{aligned} \tag{5.35}$$

$$\begin{aligned} &\leq -\frac{1}{4}\Big[d - \frac{\varrho}{2}(\varsigma_1^2 \vee \varsigma_2^2 \vee \varsigma_3^2 \vee \varsigma_4^2 \vee \varsigma_5^2)\Big]\tilde{I}^{\varrho+1} + \mathbb{J} \\ &\leq -\frac{1}{4}\Big[d - \frac{\varrho}{2}(\varsigma_1^2 \vee \varsigma_2^2 \vee \varsigma_3^2 \vee \varsigma_4^2 \vee \varsigma_5^2)\Big]\frac{1}{\chi_2^{\varrho+1}} + \mathbb{J} \leq -1. \end{aligned} \tag{5.36}$$

This can be found in Eq (5.22). Thus, $L\widetilde{\mathbb{V}} \leq -1$ at each $(\tilde{S}, \tilde{E}, \tilde{I}, \tilde{R}, \tilde{V}) \in \mathbb{F}_8$.
Case 9. We achieve, for each $(\tilde{S}, \tilde{E}, \tilde{I}, \tilde{R}, \tilde{V}) \in \mathbb{F}_9$,

$$\begin{aligned} L\widetilde{\mathbb{V}} \leq N\mathsf{c}_1\beta\tilde{I} &- \frac{1}{4}\Big[d - \frac{\varrho}{2}(\varsigma_1^2 \vee \varsigma_2^2 \vee \varsigma_3^2 \vee \varsigma_4^2 \vee \varsigma_5^2)\Big]\tilde{R}^{\varrho+1} \\ &- \frac{1}{4}\Big[d - \frac{\varrho}{2}(\varsigma_1^2 \vee \varsigma_2^2 \vee \varsigma_3^2 \vee \varsigma_4^2 \vee \varsigma_5^2)\Big]\tilde{I}^{\varrho+1} \\ &+ \nu_r + 2d + Q + l + \omega + B + \frac{\varsigma_2^2}{2} + \frac{\varsigma_1^2}{2} + \frac{\varsigma_4^2}{2} + \frac{\varsigma_5^2}{2} \end{aligned} \tag{5.37}$$

$$\begin{aligned} &\leq -\frac{1}{4}\Big[d - \frac{\varrho}{2}(\varsigma_1^2 \vee \varsigma_2^2 \vee \varsigma_3^2 \vee \varsigma_4^2 \vee \varsigma_5^2)\Big]\tilde{R}^{\varrho+1} + \mathbb{J} \\ &\leq -\frac{1}{4}\Big[d - \frac{\varrho}{2}(\varsigma_1^2 \vee \varsigma_2^2 \vee \varsigma_3^2 \vee \varsigma_4^2 \vee \varsigma_5^2)\Big]\frac{1}{\chi_3^{\varrho+1}} + \mathbb{J} \leq -1. \end{aligned} \tag{5.38}$$

This is implied by Eq (5.23). Hence, at any $(\tilde{S}, \tilde{E}, \tilde{I}, \tilde{R}, \tilde{V}) \in \mathbb{F}_9$, $L\widetilde{\mathbb{V}} \leq -1$.
Case 10. For each $(\tilde{S}, \tilde{E}, \tilde{I}, \tilde{R}, \tilde{V}) \in \mathbb{F}_{10}$, we obtain

$$\begin{aligned} L\widetilde{\mathbb{V}} \leq N\mathsf{c}_1\beta\tilde{I} &- \frac{1}{4}\Big[d - \frac{\varrho}{2}(\varsigma_1^2 \vee \varsigma_2^2 \vee \varsigma_3^2 \vee \varsigma_4^2 \vee \varsigma_5^2)\Big]\tilde{V}^{\varrho+1} \\ &- \frac{1}{4}\Big[d - \frac{\varrho}{2}(\varsigma_1^2 \vee \varsigma_2^2 \vee \varsigma_3^2 \vee \varsigma_4^2 \vee \varsigma_5^2)\Big]\tilde{I}^{\varrho+1} \\ &+ \nu_r + 2d + Q + l + \omega + B + \frac{\varsigma_2^2}{2} + \frac{\varsigma_1^2}{2} + \frac{\varsigma_4^2}{2} + \frac{\varsigma_5^2}{2}. \end{aligned} \tag{5.39}$$

$$\begin{aligned} &\leq -\frac{1}{4}\Big[d - \frac{\varrho}{2}(\varsigma_1^2 \vee \varsigma_2^2 \vee \varsigma_3^2 \vee \varsigma_4^2 \vee \varsigma_5^2)\Big]\tilde{V}^{\varrho+1} + \mathbb{J} \\ &\leq -\frac{1}{4}\Big[d - \frac{\varrho}{2}(\varsigma_1^2 \vee \varsigma_2^2 \vee \varsigma_3^2 \vee \varsigma_4^2 \vee \varsigma_5^2)\Big]\frac{1}{\chi_4^{\varrho+1}} + \mathbb{J} \leq -1. \end{aligned} \tag{5.40}$$

This implies from Eq (5.24). Hence, at any $(\tilde{S}, \tilde{E}, \tilde{I}, \tilde{R}, \tilde{V}) \in \mathbb{F}_1 0$, $L\widetilde{\mathbb{V}} \leq -1$.

Similarly, we can show that Result (*ii*) of Lemma 1 will be satisfied. According to the findings, there is one stationary distribution *pi*(.). of the model (3.1) .

6. Construction of the asymptotical extinction

The phenomenon of extinction in stochastic models refers to the state in which the entire population or system ceases to exist or diminishes to zero. This occurrence is observed in various stochastic models, including those in epidemiology, ecology, and finance. In an epidemiological model, the extinction of a disease signifies its complete eradication from the population, resulting in no remaining infected individuals. In an ecological model, species extinction indicates the complete disappearance of a population, leading to its absence in the ecosystem. Similarly, in financial models, the extinction of a company or financial instrument signifies its loss of value or viability. Studying the factors that contribute to the extinction of stochastic models is essential for policymakers and researchers to develop effective strategies that mitigate or prevent the consequences of an happening like this. The following lemmas provide insight into the reduction or disappearance of epidemics.

Lemma 6.1. *Assume that $\mathbb{M}^* = \{\mathbb{M}^*_t\}_{t\geq 0}$ is a real-valued continuous locally martingale vanish at $t = 0$. Consequently, we obtain*

- $\lim\limits_{t\to\infty} \langle \mathbb{M}^*, \mathbb{M}^* \rangle_t = \infty \quad \to \quad \lim\limits_{t\to\infty} \frac{\mathbb{M}^*_t}{\langle \mathbb{M}^*, \mathbb{M}^* \rangle_t} = 0,$
  along with,
- $\limsup\limits_{t\to\infty} \frac{\langle \mathbb{M}^*, \mathbb{M}^* \rangle_t}{t} < \infty \quad \to \quad \lim\limits_{t\to\infty} \frac{\mathbb{M}^*_t}{t} = 0,$

where $\langle \mathbb{M}^*, \mathbb{M}^* \rangle_t$ represents the quadratic variation of $\mathbb{M}^*$.

Lemma 6.2. *Assume that $(\tilde{S}, \tilde{E}, \tilde{I}, \tilde{R}, \tilde{V})$ is a solution of the model (3.1) with under the initial solution $(\tilde{S}(0), \tilde{E}(0), \tilde{I}(0), \tilde{R}(0), \tilde{V}(0)) \in \mathbb{R}^5_+$.Then, it folows*

- $\lim\limits_{t\to\infty} \frac{\tilde{S}(t)}{t} = 0, \quad \lim\limits_{t\to\infty} \frac{\tilde{R}(t)}{t} = 0. \quad \lim\limits_{t\to\infty} \frac{\tilde{I}(t)}{t} = 0, \quad \lim\limits_{t\to\infty} \frac{\tilde{E}(t)}{t} = 0, \quad \lim\limits_{t\to\infty} \frac{\tilde{V}(t)}{t} = 0,$
  Moreover, whenever $d > \frac{\varsigma_1^2 \vee \varsigma_2^2 \vee \varsigma_3^2 \vee \varsigma_4^2 \vee \varsigma_5^2}{2}$; subsequently
- $\lim\limits_{t\to\infty} \frac{\int_0^t \tilde{S}(e)dB_1(e)}{t} = 0, \quad \lim\limits_{t\to\infty} \frac{\int_0^t \tilde{I}(e)dB_3(e)}{t} = 0, \quad \lim\limits_{t\to\infty} \frac{\int_0^t \tilde{E}(e)dB_2(e)}{t} = 0,$
  $\lim\limits_{t\to\infty} \frac{\int_0^t \tilde{R}(e)dB_4(e)}{t} = 0, \quad \lim\limits_{t\to\infty} \frac{\int_0^t \tilde{V}(e)dB_5(e)}{t} = 0.$

Theorem 6.3. *Whenever $d > \frac{\varsigma_1^2 \vee \varsigma_2^2 \vee \varsigma_3^2 \vee \varsigma_4^2 \vee \varsigma_5^2}{2}$ and $R_0^s < 1$, the solution of (3.1) obeys the following conditions:*

$$\begin{aligned} &\limsup_{t\to\infty} \frac{1}{t} \ln(\kappa(\tilde{E} + \tilde{I}) + (\kappa + d + l)\tilde{R}) \\ &\leq \Psi + (\nu_r + \Lambda\nu)(\kappa + d + l) - \frac{1}{2(\kappa)^2}\left\{\kappa^2 \frac{\varsigma_3^2}{2} \wedge (\kappa(d + l) + \frac{\varsigma_2^2}{2}) \wedge (\kappa + d + l)^2(d + \omega + \frac{\varsigma_4^2}{2})\right\} < 0, \end{aligned} \tag{6.1}$$

and $\lim\limits_{t\to\infty} \left\langle \tilde{S} \right\rangle = \frac{\Lambda}{d}$ a.s.

Proof. By applying the Itô's formula to $U(t) = \kappa(\tilde{E} + \tilde{I}) + (\kappa + d + l)\tilde{R} + \lambda\tilde{V}$, we obtain

$$\begin{aligned} d\ln U(t) = &\Big\{\frac{1}{\kappa(\tilde{E}+\tilde{I}) + (\kappa+d+l)\tilde{R} + \lambda\tilde{V}} \times \Big[\kappa\psi\tilde{S}\,\tilde{I}(t-\tau) - \kappa(d+l)\tilde{E} + (\kappa+d+l)\Lambda\nu \\ &+ (\kappa+d+l)\nu_r\tilde{S} - (d+\omega)(\kappa+d+l)\tilde{R} + \lambda\eta\tilde{S} - \lambda(\sigma+d)\tilde{V}\Big] \\ &- \frac{\kappa^2\varsigma_2^2\tilde{E}^2 + \kappa^2\varsigma_3^2\tilde{I}^2 + (\kappa+d+l)^2\varsigma_4^2\tilde{R}^2 + \lambda^2\varsigma_5^2\tilde{V}^2}{2(\kappa(\tilde{E}+\tilde{I}) + (\kappa+d+l)\tilde{R} + \lambda\tilde{V})^2}\Big\}dt \\ &+ \frac{\kappa\varsigma_2\tilde{E}}{\kappa(\tilde{E}+\tilde{I}) + (\kappa+d+l)\tilde{R} + \lambda\tilde{V}}dB_2 + \frac{\kappa\varsigma_3\tilde{I}}{\kappa(\tilde{E}+\tilde{I}) + (\kappa+d+l)\tilde{R} + \lambda\tilde{V}}dB_3 \\ &+ \frac{(\kappa+d+l)\varsigma_4\tilde{R}}{\kappa(\tilde{E}+\tilde{I}) + (\kappa+d+l)\tilde{R} + \lambda\tilde{V}}dB_4 + \frac{\lambda\varsigma_5\tilde{V}}{\kappa(\tilde{E}+\tilde{I}) + (\kappa+d+l)\tilde{R} + \lambda\tilde{V}}dB_5 \end{aligned} \tag{6.2}$$

$$\begin{aligned} &\le (\psi + (\kappa+d+l)\nu_r + \lambda\eta)\tilde{S}\,dt - \frac{1}{\kappa(\tilde{E}+\tilde{I}) + (\kappa+d+l)\tilde{R} + \lambda\tilde{V}}\Big\{\kappa^2\frac{\varsigma_3^2}{2}\tilde{I}^2 \\ &+ \left(\kappa^2(d+l) + \frac{\varsigma_2^2}{2}\right)\tilde{E}^2 + (\kappa+d+l)^2\left(d+\omega+\frac{\varsigma_4^2}{2}\right)\tilde{R}^2 + \lambda^2\left(\sigma+d+\frac{\varsigma_5^2}{2}\right)\tilde{V}^2\Big\}dt \\ &+ \frac{\kappa\varsigma_2\tilde{E}}{\kappa(\tilde{E}+\tilde{I}) + (\kappa+d+l)\tilde{R} + \lambda\tilde{V}}dB_2 + \frac{\kappa\varsigma_3\tilde{I}}{\kappa(\tilde{E}+\tilde{I}) + (\kappa+d+l)\tilde{R} + \lambda\tilde{V}}dB_3 \\ &+ \frac{(\kappa+d+l)\varsigma_4\tilde{R}}{\kappa(\tilde{E}+\tilde{I}) + (\kappa+d+l)\tilde{R} + \lambda\tilde{V}}dB_4 + \frac{\lambda\varsigma_5\tilde{V}}{\kappa(\tilde{E}+\tilde{I}) + (\kappa+d+l)\tilde{R} + \lambda\tilde{V}}dB_5 \end{aligned} \tag{6.3}$$

$$\begin{aligned} &\le (\psi + (\kappa+d+l)\nu_r + \lambda\eta)\tilde{S}\,dt - \frac{1}{2(\kappa)^2}\Big\{\kappa^2\frac{\varsigma_3^2}{2} \wedge \left(\kappa^2(d+l) + \frac{\varsigma_2^2}{2}\right) \\ &\wedge (\kappa+d+l)^2\left(d+\omega+\frac{\varsigma_4^2}{2}\right) \wedge \lambda^2\left(\sigma+d+\frac{\varsigma_5^2}{2}\right)\Big\}dt \\ &+ \frac{\kappa\varsigma_2\tilde{E}}{\kappa(\tilde{E}+\tilde{I}) + (\kappa+d+l)\tilde{R} + \lambda\tilde{V}}dB_2 + \frac{\kappa\varsigma_3\tilde{I}}{\kappa(\tilde{E}+\tilde{I}) + (\kappa+d+l)\tilde{R} + \lambda\tilde{V}}dB_3 \\ &+ \frac{(\kappa+d+l)\varsigma_4\tilde{R}}{\kappa(\tilde{E}+\tilde{I}) + (\kappa+d+l)\tilde{R} + \lambda\tilde{V}}dB_4 + \frac{\lambda\varsigma_5\tilde{V}}{\kappa(\tilde{E}+\tilde{I}) + (\kappa+d+l)\tilde{R} + \lambda\tilde{V}}dB_5. \end{aligned} \tag{6.4}$$

We have, from the model (3.1),

$$\begin{aligned} d(\tilde{S}+\tilde{E}+\tilde{I}+\tilde{R}+\tilde{V}) = &\Big[\Lambda - d(\tilde{S}+\tilde{E}+\tilde{I}+\tilde{R}+\tilde{V}) - l\tilde{E} - l\tilde{I} - \sigma\tilde{V}\Big]dt \\ &+ \varsigma_1\tilde{S}\,dB_1 + \varsigma_2\tilde{E}dB_2 + \varsigma_3\tilde{I}dB_3 + \varsigma_4\tilde{R}dB_4 + \varsigma_5\tilde{V}dB_5. \end{aligned} \tag{6.5}$$

By integral the previous equation from 0 to t, we obtain

$$\left\langle \tilde{S}+\tilde{E}+\tilde{I}+\tilde{R}+\tilde{V} \right\rangle = \frac{\Lambda}{d} + ¥_2(t), \tag{6.6}$$

where

$$\begin{aligned}\text{¥}_1 = \frac{1}{d}\Big[&\frac{1}{t}(\tilde{S}(0)+\tilde{E}(0)+\tilde{I}(0)+\tilde{R}(0)+\tilde{V}(0)) - \frac{1}{t}(\tilde{S}(t)+\tilde{E}(t)+\tilde{I}(t)+\tilde{R}(t)+\tilde{V}(t))\\ &- l\frac{\int_0^t \tilde{E}(e)de}{t} - l\frac{\int_0^t \tilde{I}(e)de}{t} - \sigma\frac{\int_0^t \tilde{V}(e)de}{t}\\ &+ \frac{\varsigma_1\int_0^t \tilde{S}(e)dB_1}{t} + \frac{\varsigma_2\int_0^t \tilde{E}(e)dB_2}{t} + \frac{\varsigma_3\int_0^t \tilde{I}(e)dB_3}{t} + \frac{\varsigma_4\int_0^t \tilde{R}(e)dB_4}{t} + \frac{\varsigma_5\int_0^t \tilde{V}(e)dB_5}{t}\Big].\end{aligned} \tag{6.7}$$

By utilizing Lemmas 2 and 3, we obtain $\lim_{t\to\infty} \text{¥}_1(t) = 0$ a.s.

Thus,

$$\limsup_{t\to\infty}\left\langle \tilde{S}+\tilde{E}+\tilde{I}+\tilde{R}+\tilde{V}\right\rangle = \frac{\Lambda}{d} \quad a.s. \tag{6.8}$$

We achieves through integration of Eq (5.40),

$$\begin{aligned}\frac{\ln U(t)}{t} \le &\Big(\psi + (\nu_r+\Lambda\nu)(\kappa+d+l+\sigma)\Big)\\ &- \frac{1}{2(\kappa)^2}\Big\{\kappa_2^2\frac{\varsigma_3^2}{2} \wedge (\kappa^2(d+l+\sigma)+\frac{\varsigma_2^2}{2})\\ &\wedge (\kappa+d+l+\sigma)^2(d+\omega+\frac{\varsigma_4^2}{2})\Big\} + \text{¥}_2(t),\end{aligned} \tag{6.9}$$

where

$$\begin{aligned}\text{¥}_2(t) = &\frac{\ln U(0)}{t} + \frac{\kappa\varsigma_2}{t}\int_0^t\Big(\frac{\tilde{E}(e)}{\kappa(\tilde{E}+\tilde{I}+\tilde{V})+(\kappa+d+l+\sigma)\tilde{R}}dB_2\Big)\\ &+ \frac{\kappa\varsigma_3}{t}\int_0^t\Big(\frac{\tilde{I}(e)}{\kappa(\tilde{E}+\tilde{I}+\tilde{V})+(\kappa+d+l+\sigma)\tilde{R}}dB_3\Big)\\ &+ \frac{(\kappa+d+l+\sigma)\varsigma_4}{t}\int_0^t\Big(\frac{\tilde{R}(e)}{\kappa(\tilde{E}+\tilde{I}+\tilde{V})+(\kappa+d+l+\sigma)\tilde{R}}dB_4\Big)\\ &+ \frac{\kappa\varsigma_5}{t}\int_0^t\Big(\frac{\tilde{V}(e)}{\kappa(\tilde{E}+\tilde{I}+\tilde{V})+(\kappa+d+l+\sigma)\tilde{R}}dB_5\Big).\end{aligned} \tag{6.10}$$

Again, from Lemmas 2 and 3, we achieve

$$\lim_{t\to\infty}\text{¥}_3(t) = 0 \quad a.s.$$

As $R_0^s < 1$, we achieve, by taking the upper limit of (46),

$$\begin{aligned}\limsup_{t\to\infty}\frac{\ln U(t)}{t} \le &(\psi + (\nu_r+\Lambda\nu)(\kappa+d+l+\sigma))\\ &- \frac{1}{2(\kappa)^2}\Big\{\kappa^2\frac{\varsigma_3^2}{2} \wedge (\kappa^2(d+l+\sigma)+\frac{\varsigma_2^2}{2})\\ &\wedge (\kappa+d+l+\sigma)^2(d+\omega+\frac{\varsigma_4^2}{2}) \wedge (\kappa^2(d+l+\sigma)+\frac{\varsigma_5^2}{2})\Big\}\\ &< 0.\end{aligned} \tag{6.11}$$

This shows that

$$\lim_{t\to\infty}\tilde{E}(t)=0,\quad \lim_{t\to\infty}\tilde{I}(t)=0,\quad \lim_{t\to\infty}\tilde{R}(t)=0,\quad \text{and}\quad \lim_{t\to\infty}\tilde{V}(t)=0\quad \text{a.s.},$$

which shows that the disease I will vanish with probability one. Consequently, follows the desired asymptotical result $\lim_{t\to\infty}\langle S\rangle=\frac{\Lambda}{d}\ \ a.s.$

7. Machine learning-based computational results and analysis

In this section, we present the numerical solutions for three different cases of the $\tilde{S}\tilde{E}\tilde{I}\tilde{R}\tilde{V}$ epidemic model using Bayesian regularization neural networks (BRNNs). The numerical solutions are computed on the basis of three distinct initial conditions, as outlined in Table 2. These initial conditions allow for a comparative analysis of the model's behavior under varying outbreak scenarios.

The BRNN approach ensures stability and robustness in the estimation process, effectively minimizing overfitting and improving generalization. The numerical representations of the solutions illustrate the dynamic evolution of susceptible, exposed, infected, and recovered populations over time.

Except for the initial conditions, the remaining model parameters are kept constant throughout the simulations. These parameter values are chosen on the basis of epidemiological considerations and previous studies to reflect realistic transmission dynamics. The results are then analyzed to assess the BRNN method's efficiency in approximating the epidemic model's underlying dynamics. $\Lambda = 0.10$, $\nu = 0.231$, $\omega = 0.021$, $\psi = 0.312$, $\nu_r = 0.021$, $d = 0.123$, $Q = 0.051$, $l = 0.612$, $k = 0.351$, $\eta = 0.213$, $\sigma = 0.519$ [21].

Table 2. Initial values for model (3.1).

	Case 1	Case 2	Case 3
$\tilde{S}_0$	0.58	0.53	0.50
$\tilde{E}_0$	0.48	0.45	0.41
$\tilde{I}_0$	0.38	0.33	0.10
$\tilde{R}_0$	0.28	0.25	0.21
$\tilde{V}_0$	0.18	0.13	0.10

Table 3. The differential model of $\tilde{S}\tilde{E}\tilde{I}\tilde{R}\tilde{V}$ is evaluated using the $L-MBNNs$ method.

Case	MSE		Gradient	Performance	Epoch	Mu
	Training	Testing				
1	4.7721×10^{-11}	5.5539×10^{-11}	1.18×10^{-11}	8.06×10^{-11}	38	1
2	6.6757×10^{-11}	5.0981×10^{-11}	9.12×10^{-08}	2.41×10^{-11}	9	1
3	8.6824×10^{-12}	4.2394×10^{-11}	5.54×10^{-08}	7.67×10^{-12}	11	1

Table 3 presents the matching training procedures employed in the study. The ST values derived from the dynamic $\tilde{S}\tilde{E}\tilde{I}\tilde{R}\tilde{V}$ epidemic model's optimal performances are displayed in Figure 1. The BRNNs form the basis for the ST and the mean squared error (MSE) output performances of the dynamical $\tilde{S}\tilde{E}\tilde{I}\tilde{R}\tilde{V}$ epidemic model. These performances are based on the validation, training, and

best curves plotted in Figure 1(a),(c),(e). The best validation values for solving the nonlinear $SEIR$ epidemic model are obtained at Epochs 38, 9, and 11, with values of 8.056×10^{-11}, 2.4091×10^{-11}, and 7.6716×10^{-12}, respectively.

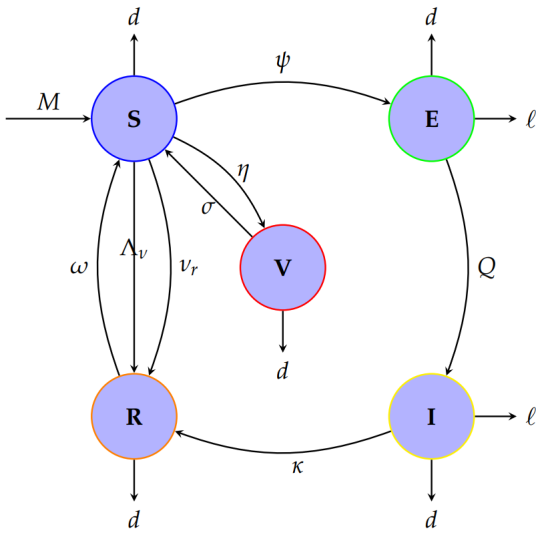

Figure 1. A compartmental model showing the transitions among the susceptible (S), exposed (E), infected (I), recovered (R), and vaccinated (V) populations.

Figure 1(b),(d),(f) authenticates the gradient measures using BRNNs to solve the dynamic $\tilde{S}\tilde{E}\tilde{I}\tilde{R}$ epidemic model. The gradient performances are recorded as 1.1775×10^{-08}, 9.1182×10^{-08}, and 5.5444×10^{-08}. These results detail the Bayesian regularization process and the accuracy of an artificial neural network (ANN) procedures for the dynamical form of the $\tilde{S}\tilde{E}\tilde{I}\tilde{R}\tilde{V}$ epidemic model.

Figure 2(a),(c),(e) displays the evaluations of the results-based authentication targets, training outputs, error curves, test scores, and fitness.

Figure 2(b),(d),(f) for the dynamical $\tilde{s}\tilde{E}\tilde{I}\tilde{R}\tilde{V}$ epidemic model illustrates zero-error performances through the Epidemic Hypotheses (EH) testing, trainning, and authentication values. The EHs are represented as -6.5×10^{-07}, -4.6×10^{-07}, and -2.5×10^{-07} for the dynamical form of the $\tilde{S}\tilde{E}\tilde{I}\tilde{R}\tilde{V}$ epidemic system.

Figure 3 employs the training, authentication, and test measures for the dynamic $\tilde{S}\tilde{E}\tilde{I}\tilde{R}\tilde{V}\tilde{V}$ epidemic model to validate the correlation operator values. The correlation is reported as a perfect representation of the model. The Mean Squared Error (MSE) convergence reflects the model's complexity by incorporating generation, testing, backpropagation, authentication, and training phases within the BRNNs framework. A comprehensive summary of these results is provided in Table 2, highlighting their effectiveness in solving the dynamic $\tilde{S}\tilde{E}\tilde{I}\tilde{R}\tilde{V}$ epidemic model.

Comparative evaluations for the dynamic $\tilde{S}\tilde{E}\tilde{I}\tilde{R}$ epidemic model are shown in Figures 4 and 5. The ANN procedures utilize Bayesian regularization and absolute error (AE) measure comparisons. Figure 4 highlights the accuracy of the BRNN scheme for different variations of the dynamical $SEIRV$ epidemic system. Figure 5 further validates the AE values for each dynamic variation of $SEIR$ epidemic model.

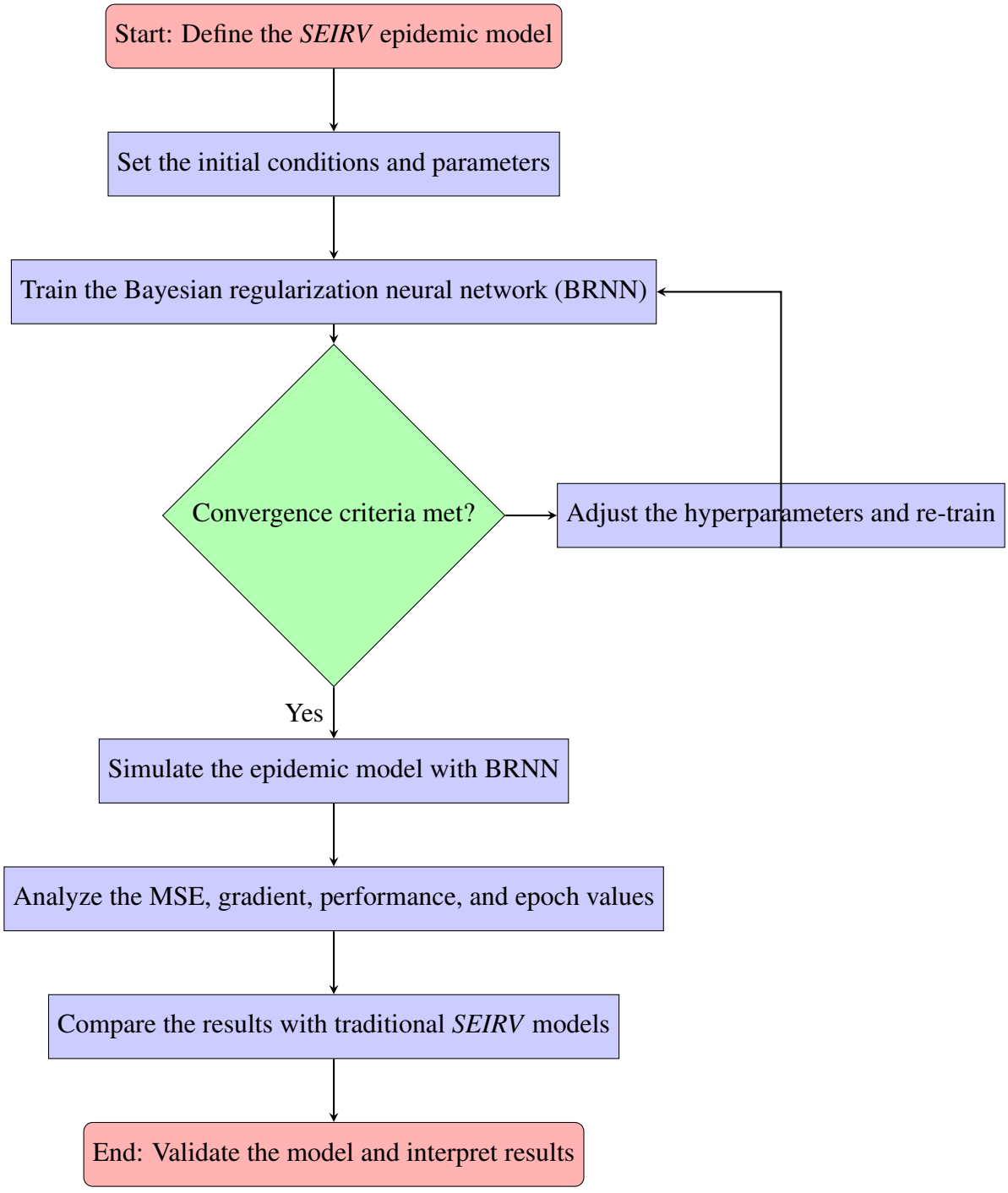

Figure 2. Flowchart of the BRNN application to *SEIRV* epidemic model.

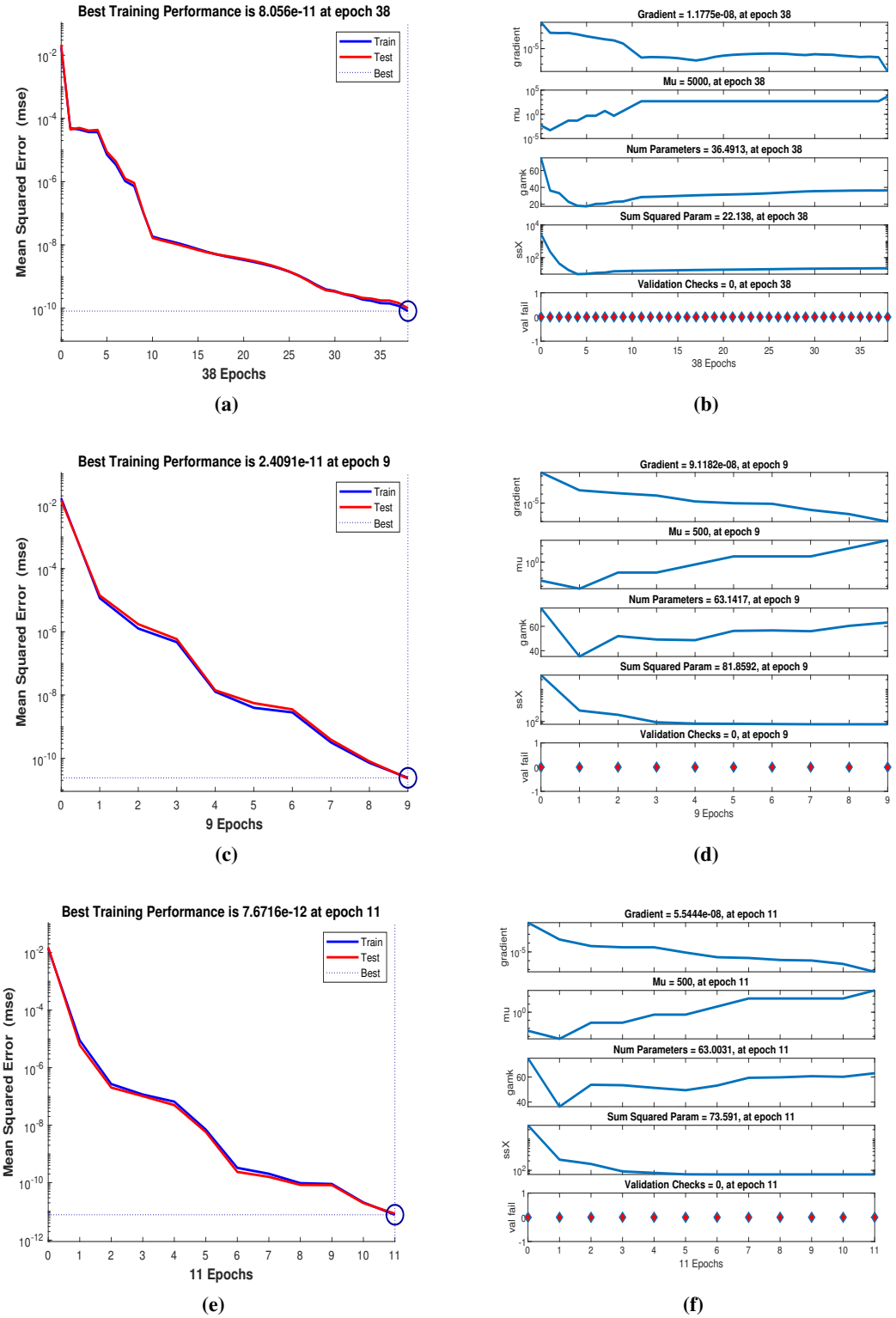

Figure 3. The dynamic $\tilde{S}\tilde{E}\tilde{I}\tilde{R}\tilde{V}$ epidemic model's performance as solved by MSE and STs.

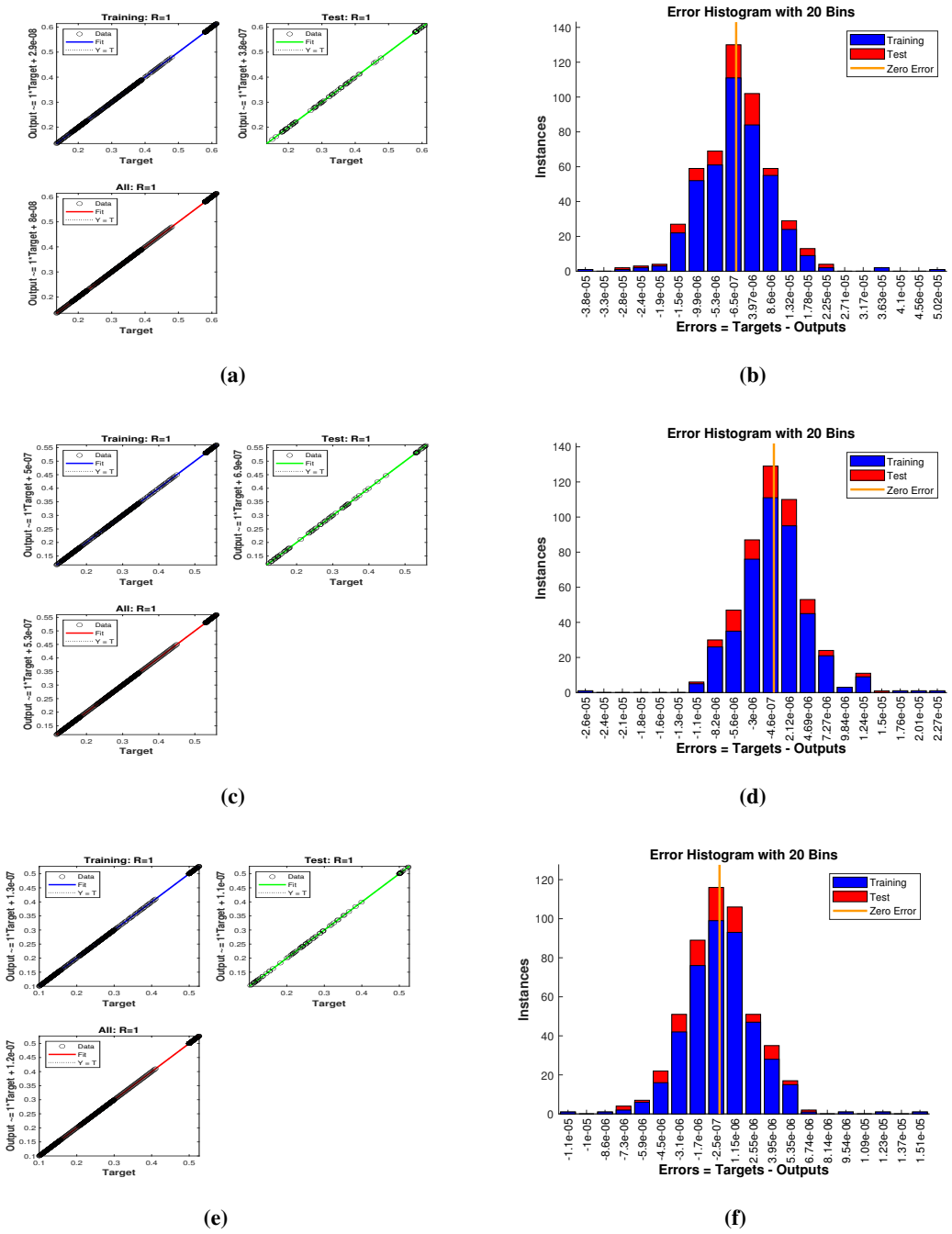

Figure 4. EH measures and estimations of the results for the dynamic $\tilde{S}\tilde{E}\tilde{I}\tilde{R}\tilde{V}$ epidemic model.

The AE measures for the dynamical $\tilde{S}\tilde{E}\tilde{I}\tilde{R}\tilde{V}$ epidemic model's special predator category $E(t)$ range from 10^{-5} to 10^{-8}, 10^{-5} to 10^{-7}, and 10^{-5} to 10^{-7} for Cases 1–3, respectively. The AE measures for the special predator category $I(t)$ range from 10^{-5} to 10^{-7}, 10^{-5} to 10^{-8}, and 10^{-5} to 10^{-9} for Cases 1–3, respectively. Similarly, the AE measures for the special predator category $\tilde{R}$ range from 10^{-4} to 10^{-6}, 10^{-5} to 10^{-8}, and 10^{-5} to 10^{-9} for Cases 1–3, respectively. These AE results confirm the accuracy

of the ANN methods using Bayesian regularization for solving the dynamical $SEIR$ epidemic model. Figures 6 and 7 present the reference solutions and the corresponding AE of the computed solutions.

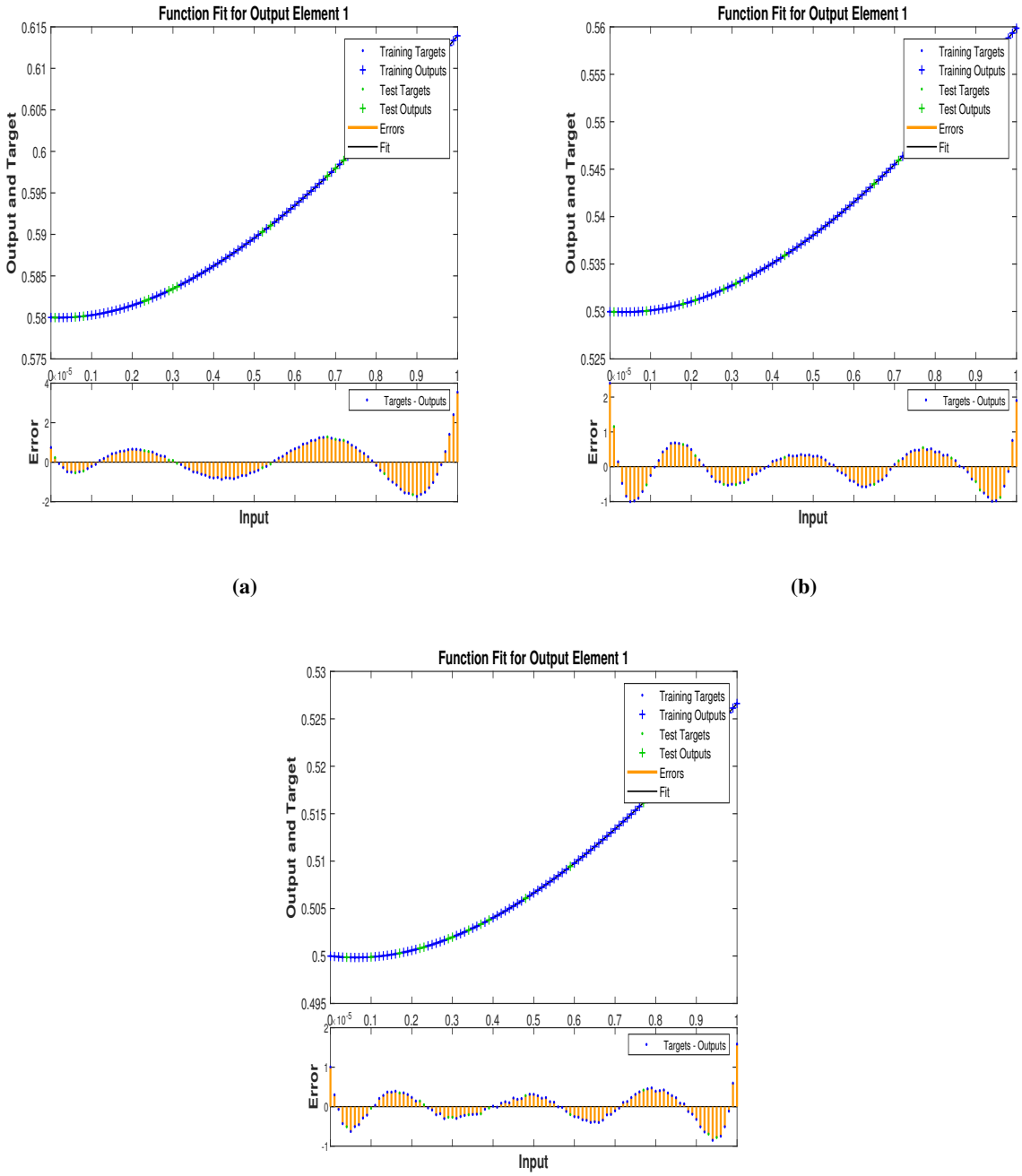

Figure 5. The performance of the regression for the dynamic $\tilde{S}\tilde{E}\tilde{I}\tilde{R}\tilde{V}$ epidemic model.

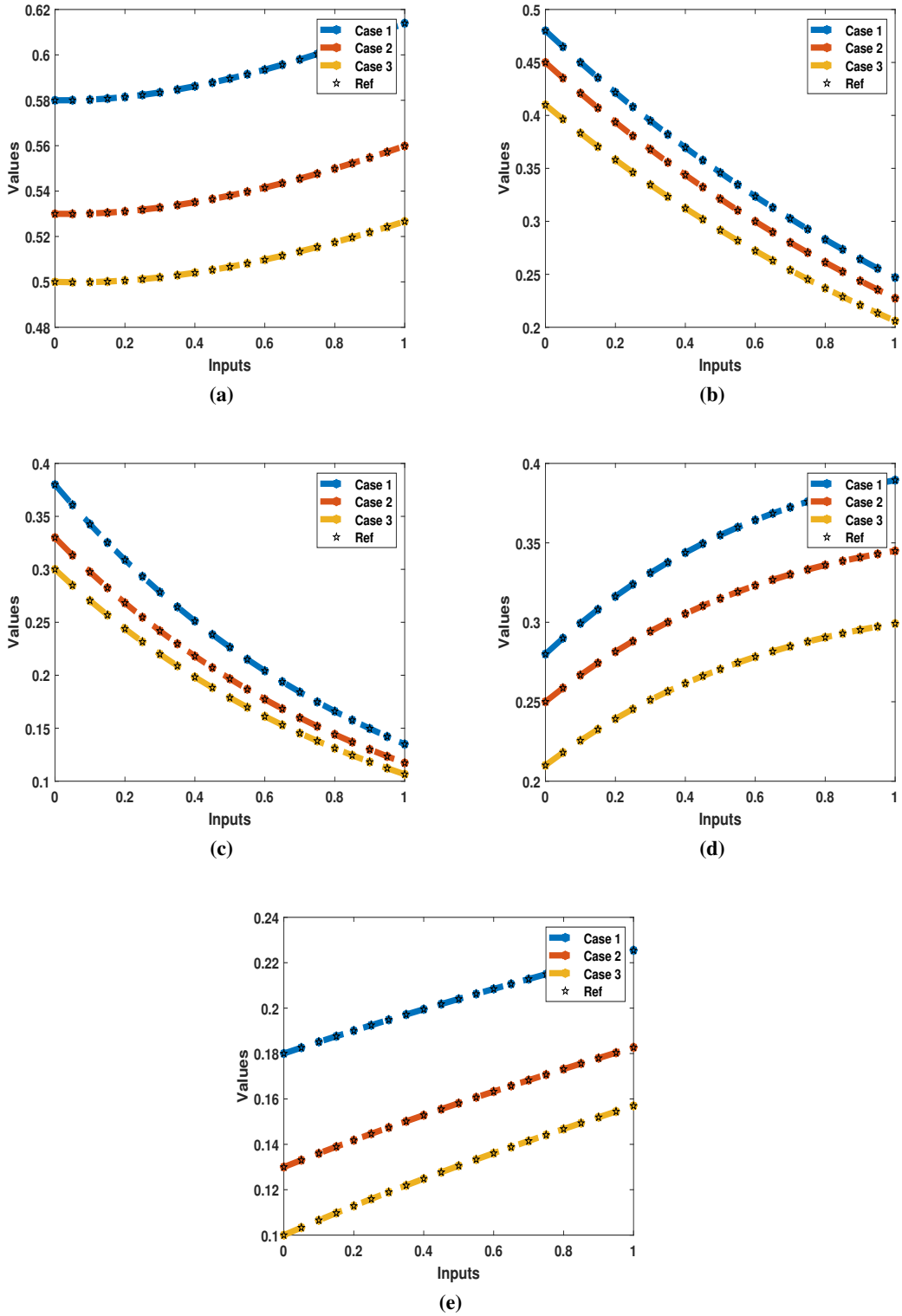

Figure 6. Achieved and reference results of the $\tilde{S}\,\tilde{E}\tilde{I}\tilde{R}\tilde{V}$ epidemic model.

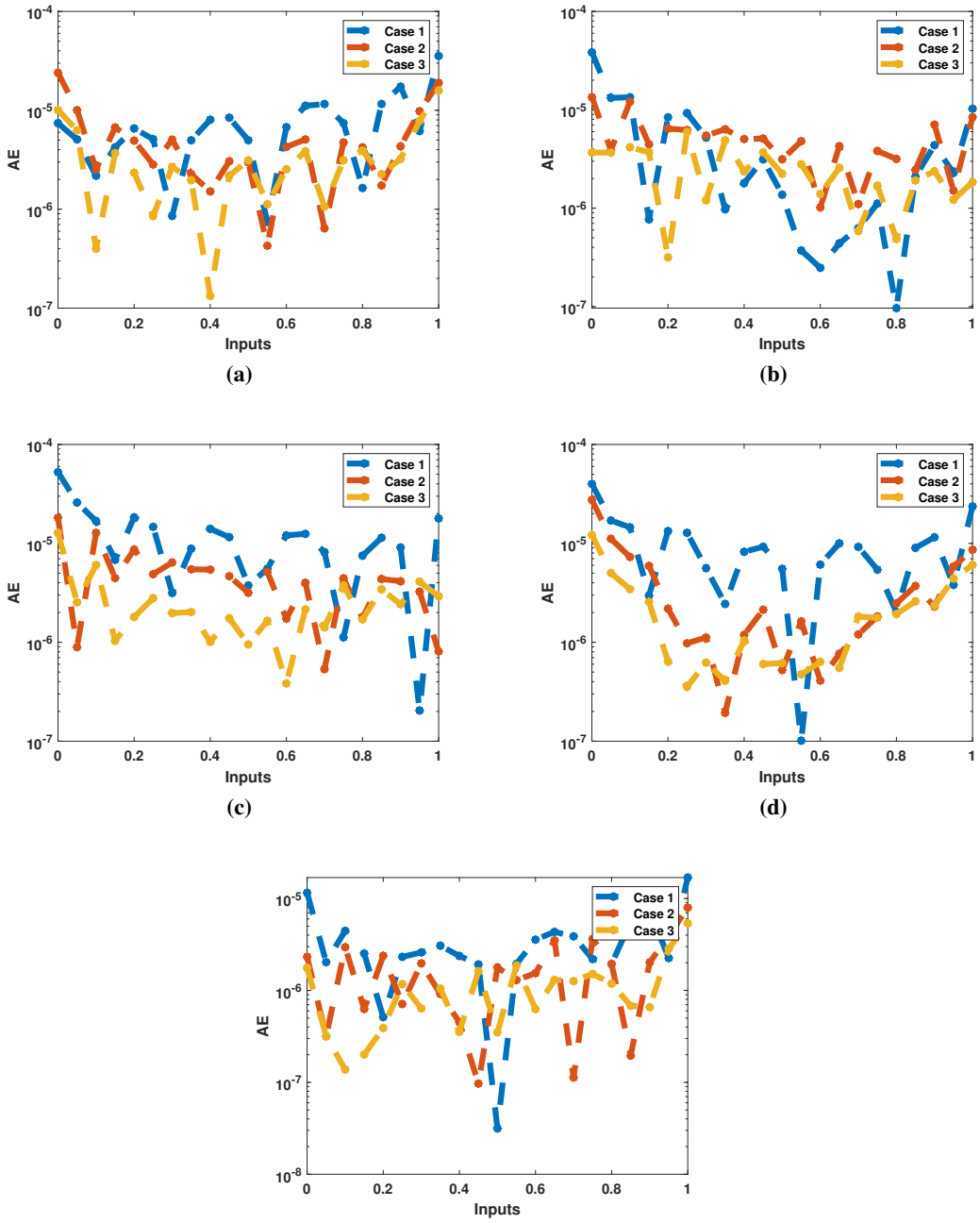

Figure 7. The values of the AE for the $\tilde{S}\,\tilde{E}\tilde{I}\tilde{R}\tilde{V}$ epidemic model.

8. Conclusions

The impact of time delay in the spread of the new coronavirus strain within the $\tilde{S}\,\tilde{E}\tilde{I}\tilde{R}\tilde{V}$ model has been analyzed using a stochastic approach. In this framework, stochastically selected agents are modeled as white Gaussian noise to account for external environmental variations. Our analysis, supported by numerical simulations, demonstrates that these stochastic influences play a crucial role

in mitigating and controlling the epidemic. The results indicate the presence of a unique stationary distribution that remains ergodic under conditions of low white noise intensity. Various visualization techniques have been employed to effectively illustrate these findings.

The stochastic $\tilde{S}\tilde{E}\tilde{I}\tilde{R}\tilde{V}$ model represents a significant advancement in understanding the epidemiological characteristics of COVID-19. By incorporating environmental noise (perturbations) and crossing immunity effects, this model provides a novel perspective on disease dynamics. Our findings suggest that the interplay between time delay and white noise significantly influences infection's disappearance while adding complexity to the system's behavior. Furthermore, we have conducted extensive numerical investigations to develop a robust stochastic computing platform based on BRNNs for solving the $\tilde{S}\tilde{E}\tilde{I}\tilde{R}\tilde{V}$ epidemic model. This computational approach enhances accuracy and stability in predicting disease progression and control measures.

9. Limitations and future work

While our model incorporates a single time delay, it may not fully capture the variability in incubation and infectious periods across individuals. Additionally, the stochasticity considered is limited, and the ANN-based simulations were trained on synthetic data rather than real-world datasets.

Future extensions of this research may include the incorporation of control variables such as vaccination strategies and targeted treatment interventions. These enhancements will provide deeper insights into epidemic control measures and further refine the predictive capabilities of the stochastic $\tilde{S}\tilde{E}\tilde{I}\tilde{R}\tilde{V}$ framework. Future work can also extend this model by incorporating multiple or distributed time delays, refining stochastic noise structures, and integrating real epidemic data for more accurate predictions.

Use of AI tools declaration

The authors declare they have not used Artificial Intelligence (AI) tools in the creation of this article.

Acknowledgments

The authors would like to thank the University of Sharjah (United Arab Emirates) for its support. This work is supported by the Research Groups on Modeling, Analysis, and Simulation of Evolutionary Problems (MASEP) and Bioinformatics and Functional Genomics (BioInformatics & FG) for the academic year 2024-2025.

Conflict of interest

The authors declare there is no conflict of interest.

References

1. W. O. Kermack, A. G. McKendrick, A contribution to the mathematical theory of epidemics, *Proc. R. Soc. London, Ser. A*, **115** (1927), 700–721. https://doi.org/10.1098/rspa.1927.0118

2. L. Billard, P. W. A. Dayananda, A multi-stage compartmental model for HIV-infected individuals: I–Waiting time approach, *Math. Biosci.*, **249** (2014), 92–101. https://doi.org/10.1016/j.mbs.2013.08.011

3. P. Pongsumpun, I. M. Tang, Dynamics of a new strain of the H1N1 influenza a virus incorporating the effects of repetitive contacts, *Comput. Math. Methods Med.*, **2014** (2014), 487974. https://doi.org/10.1155/2014/487974

4. A. Din, Y. Li, Q. Liu, Viral dynamics and control of hepatitis B virus (HBV) using an epidemic model, *Alexandria Eng. J.*, **59** (2020), 667–679. https://doi.org/10.1016/j.aej.2020.01.034

5. A. Naheed, M. Singh, D. Lucy, Numerical study of SARS epidemic model with the inclusion of diffusion in the system, *Appl. Math. Comput.*, **229** (2014), 480–498. https://doi.org/10.1016/j.amc.2013.12.062

6. R. K. Upadhyay, N. Kumari, V. S. H. Rao, Modeling the spread of bird flu and predicting outbreak diversity, *Nonlinear Anal. Real World Appl.*, **9** (2008), 1638–1648. https://doi.org/10.1016/j.nonrwa.2007.04.009

7. A. Din, Y. Li, M. A. Shah, The complex dynamics of hepatitis B infected individuals with optimal control, *J. Syst. Sci. Complexity*, **34** (2021), 1301–1323. https://doi.org/10.1007/s11424-021-0053-0

8. W. O. Kermack, A. G. McKendrick, Contributions to the mathematical theory of epidemics. II.–The problem of endemicity, *Proc. R. Soc. London, Ser. A*, **138** (1932), 55–83. https://doi.org/10.1098/rspa.1932.0171

9. J. Danane, K. Allali, Z. Hammouch, Mathematical analysis of a fractional differential model of HBV infection with antibody immune response, *Chaos, Solitons Fractals*, **136** (2020), 109787. https://doi.org/10.1016/j.chaos.2020.109787

10. A. Atangana, I. Koca, Chaos in a simple nonlinear system with Atangana-Baleanu derivatives with fractional order, *Chaos, Solitons Fractals*, **89** (2016), 447–454. https://doi.org/10.1016/j.chaos.2016.02.012

11. S. Ullah, M. Altaf Khan, M. Farooq, A new fractional model for the dynamics of the hepatitis B virus using the Caputo-Fabrizio derivative, *Eur. Phys. J. Plus*, **133** (2018), 1–14. https://doi.org/10.1140/epjp/i2018-12072-4

12. A. Din, K. Shah, A. Seadawy, H. Alrabaiah, D. Baleanu, On a new conceptual mathematical model dealing the current novel coronavirus-19 infectious disease, *Results Phys.*, **19** (2020), 103510. https://doi.org/10.1016/j.rinp.2020.103510

13. W. J. Edmunds, G. F. Medley, D. J. Nokes, The transmission dynamics and control of hepatitis B virus in the Gambia, *Stat. Med.*, **15** (1996), 2215–2233. https://doi.org/10.1002/(SICI)1097-0258(19961030)15:20<2215::AID-SIM369>3.0.CO;2-2

14. A. Khan, R. Zarin, G. Hussain, A. H. Usman, U. W. Humphries, J. F. Gomez-Aguilar, Modeling and sensitivity analysis of HBV epidemic model with convex incidence rate, *Results Phys.*, **22** (2021), 103836. https://doi.org/10.1016/j.rinp.2021.103836

15. A. Din, Y. Li, Controlling heroin addiction via age-structured modeling, *Adv. Differ. Equ.*, **521** (2020), 1–17. https://doi.org/10.1186/s13662-020-02983-5

16. T. Khan, G. Zaman, Classification of different hepatitis B infected individuals with saturated incidence rate, *Springerplus*, **5** (2016), 1082. https://doi.org/10.1186/s40064-016-2706-3

17. A. Din, Y. Li, T. Khan, G. Zaman, Mathematical analysis of spread and control of the novel corona virus (COVID-19) in China, *Chaos, Solitons Fractals*, **141** (2020), 110286. https://doi.org/10.1016/j.chaos.2020.110286

18. G. Hussain, A. Khan, M. Zahri, G. Zaman, Ergodic stationary distribution of stochastic epidemic model for HBV with double saturated incidence rates and vaccination, *Chaos, Solitons Fractals*, **160** (2022), 112195. https://doi.org/10.1016/j.chaos.2022.112195

19. Y. M. Marwa, I. S. Mbalawata, S. Mwalili, W. M. Charles, Stochastic dynamics of cholera epidemic model: Formulation, analysis and numerical simulation, *J. Appl. Math. Phys.*, **7** (2019), 1097–1125. https://doi.org/10.4236/jamp.2019.75084

20. Y. Qian, É. Marty, A. Basu, E. B. O'Dea, X. Wang, S. Fox, et al., Physics-informed deep learning for infectious disease forecasting, preprint, arXiv:2501.

21. X. Chen, J. Cao, J. H. Park, J. Qiu, Stability analysis and estimation of domain of attraction for the endemic equilibrium of an SEIQ epidemic model, *Nonlinear Dyn.*, **87** (2017), 975–985. https://doi.org/10.1007/s11071-016-3092-7

22. A. Din, Y. Li, Lévy noise impact on a stochastic hepatitis B epidemic model under real statistical data and its fractal–fractional Atangana–Baleanu order model, *Phys. Scr.*, **96** (2021), 124008. https://doi.org/10.1088/1402-4896/ac1c1a

23. A. Atangana, S. İ. Araz, New concept in calculus: Piecewise differential and integral operators, *Chaos, Solitons Fractals*, **145** (2021), 110638. https://doi.org/10.1016/j.chaos.2020.110638

24. A. Khan, G. Hussain, M. Zahri, G. Zaman, U. Wannasingha Humphries, A stochastic SACR epidemic model for HBV transmission, *J. Biol. Dyn.*, **14** (2020), 788–801. https://doi.org/10.1080/17513758.2020.1833993

25. J. Li, G. Q. Sun, Z. Jin, Pattern formation of an epidemic model with time delay, *Physica A*, **403** (2014), 100–109. https://doi.org/10.1016/j.physa.2014.02.025

26. N. Chan Chí, E. AvilaVales, G. García Almeida, Analysis of a HBV model with diffusion and time delay, *J. Appl. Math.*, **2012** (2012), 578561. https://doi.org/10.1155/2012/578561

27. A. Din, Y. Li, A. Yusuf, Delayed hepatitis B epidemic model with stochastic analysis, *Chaos, SolItions Fractals*, **146** (2021), 110839. https://doi.org/10.1016/j.chaos.2021.110839

28. O. Babasola, E. O. Omondi, K. Oshinubi, N. M. Imbusi, Stochastic delay differential equations: A comprehensive approach for understanding biosystems with application to disease modelling, *AppliedMath*, **3** (2023), 702–721. https://doi.org/10.3390/appliedmath3040037

29. Z. Bai, S. L. Wu, Traveling waves in a delayed SIR epidemic model with nonlinear incidence, *Appl. Math. Comput.*, **263** (2015), 221–232. https://doi.org/10.1016/j.amc.2015.04.048

30. Q. Liu, Q. Chen, D. Jiang, The threshold of a stochastic delayed SIR epidemic model with temporary immunity, *Physica A*, **450** (2016), 115–125. https://doi.org/10.1016/j.physa.2015.12.056

31. J. Li, Z. Teng, Bifurcations of an SIRS model with generalized non-monotone incidence rate, *Adv. Differ. Equ.*, **2018** (2018), 1–21. https://doi.org/10.1186/s13662-018-1675-y

32. A. Din, T. Khan, Y. Li, H. Tahir, A. Khan, W. A. Khan, Mathematical analysis of dengue stochastic epidemic model, *Results Phys.*, **20** (2020), 103719. https://doi.org/10.1016/j.rinp.2020.103719

33. A. Din, Y. Li, Stationary distribution extinction and optimal control for the stochastic hepatitis B epidemic model with partial immunity, *Phys. Scr.*, **96** (2021), 074005. https://doi.org/10.1088/1402-4896/abfacc

34. T. Khan, A. Khan, G. Zaman, The extinction and persistence of the stochastic hepatitis B epidemic model, *Chaos, Solitions Fractals*, **108** (2018), 123–128. https://doi.org/10.1016/j.chaos.2018.01.036

35. R. Khasminskii, *Stochastic Stability of Differential Equations*, Springer Science & Business Media, **66** (2011). https://doi.org/10.1007/978-3-642-23280-0

AIMS Press